Effects of Bacterial Species on the Biodegradation Sequence of Saturated Hydrocarbon Compounds: Evidence from Biodegradation by Pseudomonas aeruginosa XJ16 and Acinetobacter lwoffii XJ19

Yuan Liu[1], Yunyang Wan[2], Jianfa Chen[1], Xiaoli Liu[2], Na Luo[3], and Jiajia Fei[1]

[1]College of Geosciences, China University of Petroleum (Beijing)
[2]Unconventional Gas Research Institute, China University of Petroleum (Beijing)
[3]Institute of Microbiology, Chinese Academy of Sciences

November 24, 2022

Abstract

To our knowledge, this is the first study to report the different biodegradation sequences of saturated hydrocarbon compounds by two bacteria— XJ16 and XJ19—using semiquantitative analyses of the gas chromatography–mass spectrophotometry (GC–MS) data of biodegraded oils over 90-day simulation, whcih demonstrating the effects of bacterial species on the biodegradation sequences. The general biodegradation sequence of compounds for XJ16 was similar to that reported previously: -alkanes (most easily to biodegrade) > -alkylcyclohexanes > dicyclic sesquiterpenes > steranes > hopanes. However, the general biodegradation sequence of compounds for XJ19 was different: dicyclic sesquiterpenes (most easily to biodegrade) > steranes > hopanes > -alkylcyclohexanes > -alkanes.

The total biodegradation ratios of -alkanes, -alkylcyclohexanes and dicyclic sesquiterpenes by XJ16 were 69.5%, 52.9%, and 48.3% higher than those by XJ19, respectively. The -alkane/-alkylcyclohexane biodegradation sequence for XJ16 and XJ19 were different, but the dicyclic sesquiterpene biodegradation sequences for these two bacteria were the same. However, the total biodegradation ratios of the steranes and hopanes by XJ19 were 12.64% and 18.56% higher than those by XJ16, respectively. For both strains, the biodegradation sequences of some biomarkers were as follows: Cdiastrane > Cdiastrane, C-5α(H)-homopregnane > C-5α(H)-pregnane, βαC20S > βαC20R, αβC20S > αβC20R, αααC20R > αααC20R > αααC20R, Tm > Ts and CM > CH. Moreover, preferential biodegradation of the lower-molecular-weight homologues (C > C > C > C) was observed, with R epimer over the S epimer.

Effects of Bacterial Species on the Biodegradation Sequence of Saturated Hydrocarbon Compounds: Evidence from Biodegradation by *Pseudomonas aeruginosa* XJ16 and *Acinetobacter lwoffii* XJ19

Yuan Liu[a,*], Yunyang Wan[b,*], Jianfa Chen[a], Xiaoli Liu[b], Na Luo[c], Jiajia Fei[a]

[a] State Key Laboratory of Petroleum Resources and Prospecting, College of Geosciences, China University of Petroleum (Beijing), 102249, PR China

[b] Unconventional Gas Research Institute, China University of Petroleum (Beijing), 102249, PR China

[c] Institute of Microbiology, Chinese Academy of Sciences, 100101, PR China

Abstract

To our knowledge, this is the first study to report the different biodegradation sequences of saturated hydrocarbon compounds by two bacteria—*Pseudomonas aeruginosa* XJ16 and *Acinetobacter lwoffii* XJ19—using semiquantitative analyses of the gas chromatography–mass spectrophotometry (GC–MS) data of biodegraded oils over 90-day simulation, whcih demonstrating the effects of bacterial species on the biodegradation sequences. The general biodegradation sequence of compounds for *P. aeruginosa* XJ16 was similar to that reported previously: *n*-alkanes (most easily to biodegrade) > *n*-alkylcyclohexanes > dicyclic sesquiterpenes > steranes > hopanes. However, the general biodegradation sequence of compounds for *A. lwoffi* XJ19 was different: dicyclic sesquiterpenes (most easily to biodegrade) > steranes > hopanes > *n*-alkylcyclohexanes > *n*-alkanes.

The total biodegradation ratios of *n*-alkanes, *n*-alkylcyclohexanes and dicyclic

Foundation item: National Science and Technology Major Project (2016ZX05050011, 2016ZX05040002), and National Natural Science Foundation of China (41373086)

***Corresponding author:** E-mail: liuyuandxy@163.com; wanyunyang@cup.edu.cn

sesquiterpenes by *P. aeruginosa* XJ16 were 69.5%, 52.9%, and 48.3% higher than those by *A. lwoffi* XJ19, respectively. The *n*-alkane/*n*-alkylcyclohexane biodegradation sequence for *P. aeruginosa* XJ16 and *A. lwoffi* XJ19 were different, but the dicyclic sesquiterpene biodegradation sequences for these two bacteria were the same. However, the total biodegradation ratios of the steranes and hopanes by *A. lwoffi* XJ19 were 12.64% and 18.56% higher than those by *P. aeruginosa* XJ16, respectively. For both strains, the biodegradation sequences of some biomarkers were as follows: C_{29}diastrane > C_{27}diastrane, C_{22}-5α(H)-homopregnane > C_{21}-5α(H)-pregnane, βαC_{27}20S > βαC_{27}20R, αβC_{27}20S > αβC_{27}20R, αααC_{27}20R > αααC_{28}20R > αααC_{29}20R, Tm > Ts and C_{29}M > C_{29}H. Moreover, preferential biodegradation of the lower-molecular-weight homologues (C_{31} > C_{32} > C_{33} > C_{34}) was observed, with R epimer over the S epimer.

Key words

Biodegradation sequence; Saturated hydrocarbon compounds; Biodegradation ratio; Bacterial species; *Pseudomonas aeruginosa*; *Acinetobacter lwoffii*

1. Introduction

Biodegradation of crude oil in reservoir is an important process of biogeochemical cycle in deep earth (Connan, 1984; Head et al., 2003; Andrew et al., 2010; Oldenburg et al., 2017). The effects of biodegradation on the physical and chemical properties of crude oil have always been a research hotspot in organic geochemistry and

43 geomicrobiology (Peters and Moldowan, 1993; Roling et al., 2003; Pan., 2015;
44 Agyingi et al., 2019). Following biodegradation, the density and viscosity of crude oil
45 increase; hydrocarbon compounds are consumed; nonhydrocarbon, asphaltene, sulfur,
46 and metal ion concentrations increase; acidity increases; and API (American
47 Petroleum Institute) gravity values decrease (Peters and Moldowan, 1993; Meredith et
48 al., 2000; Wenger et al., 2002). Biodegradation of crude oil is often explained as a
49 quasi-stepwise process, indicating that some compounds are less stable than others in
50 a given biomarker compound class, although these compounds may still be preserved
51 when more resistant compounds begin to be biodegraded (Peters and Moldowan,
52 2005). Bacteria do not biodegrade different compounds sequentially but instead
53 utilize different compounds at different rates simultaneously.

54 Except for biodegradation time and environmental conditions (temperature, salinity,
55 pH, and electron donors and acceptors), biodegradation primarily depends on
56 microorganisms and the chemical structure of hydrocarbons (Peters et al., 2005;
57 Larter et al., 2003, 2006; Varjani et al., 2017). Sequential and systematic variations in
58 crude oil biomarkers are commonly observed in reservoir biodegradations and
59 laboratory simulations (Koopmans et al., 2002; Jones et al., 2008; Liao et al., 2012;
60 Cheng et al., 2016; Pan et al., 2017; Huang et al., 2017; Oblasov et al., 2018).
61 Moreover, the general order of bioresistance of various biomarker compound classes
62 in saturated hydrocarbons may mostly follow the following sequence: *n*-alkanes (least
63 resistant) > acyclic isoprenoids > steranes > hopanes > diasteranes (most resistant)
64 (Seifert et al., 1979; Goodwin et al., 1983; Volkman et al., 1984; Connan, 1984; Peters

et al., 1993; Alberdi et al., 2001; Peters et al., 2005; Du et al., 2011; Pan et al., 2017). Normal alkanes are more easily biodegraded than branched alkanes, and the higher the concentrations of branched alkanes, the more difficult the crude oil is to biodegrade (Connan, 1984). Williams et al. (1986) suggested that 8β(H)-homodrimane is more easily biodegraded than 8β(H)-drimane. The bioresistance of pregnane and diastrane is stronger than that of regular sterane (Lin et al., 1989; Peters and Moldowan, 1993). Compared with C_{29}-steranes and C_{29}-diastranes, C_{27}-steranes and C_{27}-diastranes are preferentially used by microorganisms (Seifert and Moldwan, 1979). The ratio of C_{29}-sterane ββ/(αα + ββ) increases with an increasing degree of biodegradation (Peters and Moldowan, 1993). Ts/Tm increases with an increasing biodegradation level. C_{29}-17α, 21β-norhopane and $C_{32–35}$-17α,21β-homohopanes are more difficult to biodegrade than C_{31}-17α,21β-hopane. Moretane is more stable than hopane. For $C_{31–34}$-17α,21β-homohopanes, the biodegradation ratios of R-configuration homohopanes were higher than those of S-configuration homohopanes (Lin et al., 1989). However, previous studies have not confirmed the effects of bacterial species on the biodegradation sequence.

Semiquantitative evaluation of biodegradation is performed to measure the degree of biodegradation, i.e., biodegradation ratio, by determining the concentrations of the compounds in unaltered oil sources and biodegraded crude oil. The crude oil concentration can be obtained by semiquantitative GC–MS using an internal standard. It is impossible to know the exact concentrations of the compounds before

87 biodegradation and clear biological information about biodegradation in geological
88 samples. However, laboratory simulations are not influenced by complex geological
89 factors; moreover, such simulations provide biodegradation information of the entire
90 process and not just the final biodegradation results. In simulated aerobic
91 biodegradation, crude oil can be used as the unique carbon source and bacteria as the
92 degrader under optimum growth conditions of temperature, pressure, and
93 microorganism cell/oil ratio (Essaid et al., 1995; Bicalho et al., 2004; Pan et al., 2017).
94 *Pseudomonas aeruginosa* and *Acinetobacter lwoffii* can utilize hydrocarbons as
95 carbon sources and produce biosurfactants (Throne-Holst et al., 2007; Varjani et al.,
96 2016), which can greatly enhance the solubilization of petroleum hydrocarbons
97 (Aparna et al., 2012; Mnif et al., 2013). In this study, we used *P. aeruginosa* XJ16 and
98 *A. lwoffii* XJ19 (both isolated by our group from production wells in the Xinjiang
99 oilfield, China) for biodegradation simulations to calculate the biodegradation ratio
100 (%) from the concentrations (μg/g) of specific compounds in unaltered and
101 biodegraded oils using GC–MS data (Goswami and Singh, 1991; Mishra et al., 2017).
102 We further clarified the biodegradation characteristics and ultimately determined the
103 biodegradation sequences of compounds for these twobacteria. The target
104 hydrocarbons were saturated hydrocarbons, encompassing *n*-alkanes (*m*/*z* 85),
105 *n*-alkylcyclohexanes (*m*/*z* 82), bicyclic sesquiterpenes (*m*/*z* 123), the steranes (*m*/*z*
106 217), and the hopanes (*m*/*z* 191).

2. Materials and methods

2.1 Crude oil

For the biodegradation simulation, a crude oil sample was collected from a production well of Changqing Oilfield, China, with a density of 0.82 g/cm^3 (28 °C) and viscosity of 2.69 mPa·s (20 °C). Based on total ion chromatogram (TIC; Fig. 1a), this oil was not biodegraded. The relative concentrations of saturates, aromatics, resins, and asphaltenes in the sample were 77.4%, 14.9%, 5.26%, and 2.48%, respectively. These analytical tests were conducted at the State Key Laboratory of Petroleum Resources and Prospecting, China University of Petroleum (Beijing).

2.2 Bacterial isolation, screening, and identification

In this study, we isolated two strains from production wells of Xinjiang Oilfield, China, designated XJ16 and XJ19.

2.2.1 Sample source and enrichment

The produced liquid from production wells in Xinjiang Oilfield were sampled using aseptic sampling bottle. Upon collection, samples were immediately sealed, after which they were returned to the laboratory and sealed in a 4°C refrigerator until analysis. In the super-clean bench, the samples were inoculated into different liquid media and incubated at 35°C for bacterial growth. After 5–7 days of incubation, an aliquot of the cloudy sample was inoculated into a new medium, and repeat three times.

2.2.2 Bacterial isolation and screening

A small amount of bacterial liquid was inoculated into isolation medium with an aseptic inoculation ring. A line was then drawn on the plate isolation medium, covered and allowed to stand for 20–30 min so that the bacterial liquid fully infiltrated the medium. The inoculated plates were subsequently incubated at 35°C under aerobic conditions. Then, put the single colony using the aseptic gun head into the screening medium in the super-clean bench, and put it in the incubator for cultivation. The isolation/screening medium was as follows: yeast extract, 0.5 g/L; tryptone, 0.25 g/L; peptone, 0.75 g/L; glucose, 0.5 g/L; soluble starch, 0.5 g/L; K_2HPO_4, 0.3 g/L; $MgSO_4 \cdot 7H_2O$, 0.024 g/L; and sodium pyruvate, 0.3 g/L (pH adjusted to 6.5). Medium was autoclaved at 121°C for 30 min before use. Gram staining was used to observe the growth of the strain under the microscope.

2.2.3 Bacterial identification bsaed on 16S rRNA gene

Bacterial strains in the logarithmic growth phase were extracted using a bacterial deoxyribonucleic acid (DNA) extraction kit (Shanghai Biotechnicians) to extract total DNA. Nucleotide sequence of conserved segment 8-1510 of 16Sr DNA Gene were amplified using the 27F (AGAGTTTGATCMTGGCTCAG) and 1492R (TACGYTACCTTGTTACGACTT) bacterial primers. The amplification results were observed using a Sai Zhi gel imaging system. The retrieved sequences were utilized for BLAST searches of the EzTaxon-e database (http://eztaxon-e.ezbiocloud.net/). The cell morphology of the isolates was examined by scanning electron microscopy at

148 the Institute of Microbiology, Chinese Academy of Sciences. The colonies of *P.*
149 *aeruginosa* XJ16 were ellipsoidal, greyish white with smooth edges, and the cells
150 were 0.9–1.3 μm long and 0.6–0.8 μm wide (Fig. 1b). *A. lwoffii* XJ19 colonies were
151 bacilliform with regular edges and smooth, slightly raised surfaces. The cells were
152 1.2–2.5 μm long and 0.4–0.6 μm wide (Fig. 1c).

153 2.3 Aerobic biodegradation simulations

154 We used the isolated bacteria to conduct two biodegradation simulations. Briefly,
155 20 ml bacterial solution (OD_{600} of 0.8) was inoculated into 100 ml basal medium with
156 1 g crude oil from the Changqing oilfield. The basal medium comprised KNO_3 (3 g/L),
157 Na_2HPO_4 (2 g/L), KH_2PO_4 (2 g/L), $MgSO_4$ (0.5 g/L), NaCl (0.5 g/L), NH_4Cl (1 g/L),
158 and trace elements (10 ml). The trace elements included $Na_2EDTA{\cdot}2\ H_2O$ (12 g/L),
159 NaOH (2 g/L), $CaCl_2$ (1 g/L), $MnSO_4{\cdot}4\ H_2O$ (0.4 g/L), $ZnSO_4{\cdot}7\ H_2O$ (0.4 g/L),
160 H_2SO_4 (98%; 0.5 ml), Na_2SO_4 (10 g/L), $Na_2MoO_4{\cdot}2\ H_2O$ (0.1 g/L), $FeSO_4{\cdot}7H_2O$ (2
161 g/L), and $CuSO_4{\cdot}5\ H_2O$ (0.1 g/L). The samples were incubated at a constant
162 temperature (35 °C) while shaking at 120 rpm/min. Aerobic biodegradation
163 simulations were conducted for 90 days during which the samples were collected on
164 days 10, 20, 40, 60, and 90 (three replicates). An appropriate amount of
165 dichloromethane was added to the samples for sterilization and biodegraded oil
166 extraction.

167 2.4 GC–MS

168 2.4.1 Pretreatment and experimental condition

After precipitating with 30 mL n-hexane for 12 h, crude oil (about 20-30 mg) was deasphalted and then fractionated into saturated hydrocarbons, aromatic hydrocarbons, and resins by column chromatography (Du et al., 2011). First, 3 g silica and 2 g neutral alumina were placed into the chromatographic column, wetting with 5 mL petroleum ether. Then, saturated hydrocarbons were eluted 30 times using 1 mL petroleum ether, whereas aromatic hydrocarbons were eluted 25 times using a 1 mL mixture of dichloromethane and petroleum ether (2:1). Finally, the non-hydrocarbon fraction was eluted 15 times using a 1 mL mixture of dichloromethane and methanol (9:1). The total weight of the eluted fractions and asphaltenes divided by the initial loaded weight was designated as the recovery efficiency.

GC–MS analyses of saturated hydrocarbons were conducted using a Thermo Finnigan Trace-DSQ mass spectrometer coupled to an HP 6890 GC equipped with an HP-5MS column (30 m × 0.25 mm ID) with a 0.25-μm coating. Helium was used as the carrier gas. The GC oven temperature was initially set at 50 °C, after which it was increased to 120 °C at a rate of 20 °C/min, 250 °C at a rate of 4 °C/min, and 310 °C at a rate of 3 °C/min and maintained at this temperature for 30 min. The mass spectrometer was operated in the full-scan, electron impact mode with an electron energy of 70 eV.

2.4.2 Semiquantitative calculation

D-nC_{24} (10 μg) was added as the internal standard to the oil for the semiquantification of the saturated hydrocarbon fraction. The peak area was used for the calculation of concentration and molecular parameter. Response factors for the

components of interest relative to the internal standard were assumed to be 1.0, and calibration was not applied. To calculate concentration, the following formula was used:

$$\frac{C_X}{C_I} = h\frac{S_X}{S_I} \quad \text{and} \quad C_I = \frac{m_I}{m_0} \quad (1)$$

where C_X is the concentration of the compounds in crude oil (μg/g); C_I is the concentration of the internal standard; m_I and m_0 represent the internal standard quality and oil quality used in fractionation, respectively; h is the response coefficient; S_X is the peak area of each compound in crude oil; and S_I is the peak area of the internal standard.

2.4.3 Biodegradation ratio

Using the GC–MS data, we compared fresh and biodegraded crude oil to obtain information on biodegradation (Malik and Ahmed, 2012). Cx data were used to calculate the biodegradation ratio (%) based on the concentration (μg/g) of fresh and biodegraded crude oil:

$$\text{Biodegradation ratio} = \frac{C_0 - C_A}{C_0} \times 100\% \quad (2)$$

where C_0 is the concentration of compounds in fresh crude oil (μg/g) and C_A is the concentration of compounds in biodegraded crude oil (μg/g).

3. Results and discussion

3.1 Overall biodegradation characteristics

Initially, the crude oil floated on the transparent medium (Fig. 1a). As biodegradation progressed, the crude oil dispersed in the basic medium as minute particles and the medium became more turbid with an obvious emulsification phenomenon (Fig. 1d-m, after another manuscript submitted for review). On day 90, the biodegradation ratios of the crude oil for *P. aeruginosa* XJ16 and *A. lwoffii* XJ19 were 69.3% and 33.2%, respectively. In addition, biodegraded oil fractions displayed gradual changes such that the saturated fraction decreased rapidly and the aromatics, resins, and asphaltenes increased progressively (Table 1). A total ion chromatogram (TIC) of saturated hydrocarbons showed completely different biodegradation characteristics for these two bacteria at days 10, 20, 40, 60, and 90 (Fig. 1). *P. aeruginosa* XJ16 had biodegraded several compounds by day 10 and the baseline of TIC uplifted (Fig. 1d, f, h, j, l), whereas *A. lwoffii* XJ19 had not biodegraded many compounds even by day 90 (Fig. 1e, g, i, k, m).

3.2 *P. aeruginosa* XJ16 demonstrated higher biodegradation ratios of *n*-alkanes, *n*-alkylcyclohexanes, and bicyclic sesquiterpenes

Biodegraded oils were monitored during the 90-day laboratory simulation to determine the biodegradation ratios of compounds (Tables 2–4) and biodegradation sequence of biomarker compound classes. Tables 2–4 list the numbers or/and

228 abbreviations of the compounds identified in Figs 2–4.

229 3.2.1 *n*-alkanes

230 Typically, *n*-alkanes, particularly those with lower carbon numbers, are the most
231 susceptible to biodegradation. The results of the semiquantitative GC–MS analyses of
232 nC_{14}–nC_{35} are shown in Table 2 and Fig 2 (data are presented in another manuscript
233 submitted for review). The total concentration of *n*-alkanes in the presence of *P.*
234 *aeruginosa* XJ16 decreased from 93,062.3 μg/g to 1108.5 μg/g, equaling a total
235 biodegradation ratio of 98.8%. The biodegradation ratios of nC_{14}, nC_{15}, nC_{16}–nC_{26},
236 nC_{27}–nC_{28}, nC_{29}–nC_{32}, nC_{33}, and nC_{34}–nC_{35} were 99.8%, 99.4%, 99.7%–99.0%,
237 99.7%–99.0%, 98.6%–96.3%, 81.7%, and 65.7%–60.2%, respectively. Therefore, the
238 *n*-alkane biodegradation sequence was nC_{14}, nC_{15}, nC_{16}–nC_{26}, nC_{27}–nC_{28} >
239 nC_{29}–nC_{32} > nC_{33} > nC_{34}–nC_{35}. *P. aeruginosa* XJ16 could more easily biodegrade
240 *n*-alkanes with low carbon atoms than *n*-alkanes with high carbon atoms (Fig 2a). Liu
241 et al. (2012) characterized several *n*-alkane hydroxylases, including two *alkB*
242 monooxygenases (nC_{10}–nC_{20}), two P450 monooxygenases (nC_5–nC_{16}), and one
243 *almA*-like monooxygenase (>nC_{32}), in *P. aeruginosa* SJTD 21 using whole-genome
244 DNA sequencing.

245 *Acinetobacter lwoffi* can use medium- (nC_5–nC_{16}) and long-chain (>nC_{17}) alkanes
246 as carbon source (nC_{10}–nC_{20}: Alon et al., 1993; nC_{12}–nC_{28}: Amund et al., 1985). The
247 total concentration of *n*-alkanes in the presence of *A. lwoffii* XJ19 decreased from
248 93,063.3 μg/g to 65,811.1 μg/g, with a total biodegradation ratio of 29.3%; this ratio
249 was much lower than that in the presence of *P. aeruginosa* XJ16. The biodegradation

ratios of nC_{14}, nC_{15}, nC_{16}–nC_{26}, nC_{27}–nC_{28}, nC_{29}–nC_{31}, nC_{32}–nC_{33}, and nC_{34}–nC_{35} were 81.5%, 55.8%, 9.1%–34.1%, 41.4%–49.2%, 56.8%–64.9%, 73.0%–74.5%, and 62.6%–67.7%, respectively. Therefore, the *n*-alkane biodegradation sequence was nC_{14} > nC_{32}–nC_{33} > nC_{34}–nC_{35} > nC_{15}, nC_{29}–nC_{31} > nC_{27}–nC_{28} > nC_{16}–nC_{26}. In this study, the biodegradation ratios of long-chain alkanes in the presence of *A. lwoffi* XJ19 (>nC_{28}: 49.2%–74.5%) were higher than those of *n*-alkanes with 16–27 C atoms (9.1%–41.4%) (Fig 2b). Throne-Holst et al. (2007) identified *alkB* monooxygenases (nC_{10}–nC_{20}) and *almA* monooxygenase (>nC_{32}) in the *Acinetobacter* sp. strain DSM 17874. Moreover, genes encoding *almA* homologues were identified in other long-chain *n*-alkane-degrading *Acinetobacter* strains (Throne-Holst et al., 2007).

3.2.2 *n*-alkylcyclohexanes

n-alkylcyclohexanes, one of the main components of crude oil, exhibited an *m*/*z* of 82 on mass chromatograms. These are more resistant to biodegradation than *n*-alkanes (Kaplan et al., 1997). However, the published data on the mechanisms underlying the alterations/modifications of these compounds in simulated aerobic degradation are limited (Frances et al., 2002). The results of the semiquantitative GC–MS analyses of C_8–C_{31} *n*-alkylcyclohexanes are shown in Table 3 and Fig 3. The total concentration of *n*-alkylcyclohexanes in the presence of *P. aeruginosa* XJ16 decreased from 9178.0 μg/g to 262.9 μg/g, equaling a total biodegradation ratio of 97.1% (Fig 3a). The biodegradation ratios of nC_8-cHex, nC_9–nC_{25}-cHex, nC_{26}–nC_{28}-cHex, and nC_{29}–nC_{31}-cHex were 72.7%, 85.7%–99.8%, 94.3%–99.7%, and 93.1%–99.8%,

271 respectively. Therefore, the *n*-alkylcyclohexane biodegradation sequence was
272 nC_9–nC_{25}-cHex, nC_{26}–nC_{28}-cHex, nC_{29}–nC_{31}-cHex > nC_8-cHex.

273 The total concentration of *n*-alkylcyclohexanes in the presence of *A. lwoffi* XJ19
274 decreased from 9178.0 μg/g to 5114.1 μg/g, equaling a total biodegradation ratio of
275 44.3%; this ratio was lower than that in the presence of *P. aeruginosa* XJ16. The
276 biodegradation ratios of nC_8-cHex, nC_9–nC_{25}-cHex, nC_{26}–nC_{28}-cHex, and
277 nC_{29}–nC_{31}-cHex were 26.8%, 30.8%–50.4%, 47.0%–58.5%, and 68.6%–76.8%,
278 respectively. Therefore, the *n*-alkylcyclohexane biodegradation sequence was
279 nC_{31}–nC_{29}-cHex > nC_{28}–nC_{26}-cHex > nC_{25}–nC_9-cHex > nC_8-cHex. In the presence of
280 *A. lwoffi*, the biodegradation ratios of long-chain *n*-alkylcyclohexanes were higher
281 than those of short-chain *n*-alkylcyclohexanes (Fig 3b). In general, *n*-alkanes are the
282 first components to be removed and are followed by *n*-alkylcyclohexanes (Frances et
283 al., 2002); however, the biodegradation ratios of *n*-alkylcyclohexanes (44.3%) were
284 higher than those of *n*-alkanes (29.8%) in the presence of *A. lwoffi* XJ19. The
285 *Acinetobacter* sp. ODDK71 strain degrades several *n*-alkylcyclohexanes (alkyl side
286 chain length of ≥12) by cometabolism with *n*-alkane and exhibits two pathways for
287 dodecylcyclohexane degradation (Koma et al., 2003). For *A. lwoffii*,
288 n-dodecylbenzene was completely degraded via phenylacetic and homogentisic acids,
289 whereas n-tridecylbenzene was transformed via 3-phenylpropionic acid to
290 transcinnamic acid, which was the dead-end product (Amund et al., 1989).

291 ### 3.2.3 Bicyclic sesquiterpenes

Though bicyclic sesquiterpenes are a class of important biomarkers in crude oil and source rocks, only few studies have reported on their biodegradation characteristics. With the increase of degradation level, the relative percentage of bicyclic sesquiterpenes decreases continuously, indicating that they are easily biodegraded. The results of the semiquantitative GC–MS analyses of bicyclic sesquiterpenes are shown in Table 4 and Fig 4. Williams et al. (1986) suggested that 8β(H)-homodrimane is more easily biodegraded than 8β(H)-drimane. However, in this study, the biodegradation ratio of 8β(H)-drimane was higher than those of 8β(H)-homodrimane, and 8β(H)-drimane/8β(H)-homodrimane decreased with an increased biodegradation degree for both *P. aeruginosa* XJ16 and *A. lwoffi* XJ19.

The total concentration of bicyclic sesquiterpenes in the presence of *P. aeruginosa* XJ16 decreased from 1327.1 μg/g to 333.6 μg/g, equaling a total biodegradation rate of 74.9%. The biodegradation ratios of C_{14}-bicyclic sesquiterpene, C_{15}-bicyclic sesquiterpene, 8α(H)-drimane and 8β(H)-drimane, C_{15}-bicyclic and C_{16}-bicyclic sesquiterpene, and 8β(H)-homodrimane were 95.2%–97.4%, 81.5%–87.8%, 79.8%–78.5%, 63.4%–68.5%, and 60.0%, respectively. Therefore, the bicyclic sesquiterpene biodegradation sequence was C_{14}-bicyclic sesquiterpene > C_{15}-bicyclic sesquiterpene > 8α(H)-drimane, 8β(H)-drimane > C_{15}-bicyclic sesquiterpene, C_{16}-bicyclic sesquiterpene > 8β(H)-homodrimane (Fig 4a).

The total concentration of bicyclic sesquiterpenes in the presence of *A. lwoffi* XJ19 decreased from 1327.1 μg/g to 550.5 μg/g, equaling a total biodegradation ratio of 58.5%. The biodegradation ratios of C_{14}-bicyclic sesquiterpenes, C_{15}-bicyclic

sesquiterpenes, 8α(H)-drimane and 8β(H)-drimane, C_{15}-bicyclic and C_{16}-bicyclic sesquiterpene, and 8β(H)-homodrimane were 73.2%–74.9%, 61.4%–66.8%, 60.0%–62.6%, 41.7%–60.3%, and 50.5%, respectively. Therefore, the bicyclic sesquiterpene biodegradation sequence was C_{14}-bicyclic sesquiterpene > C_{15}-bicyclic sesquiterpene > 8α(H)-drimane, 8β(H)-drimane > C_{15}-bicyclic sesquiterpene, C_{16}-bicyclic sesquiterpene, 8β(H)-homodrimane (Fig 4b).

3.3 *A. lwoffii* XJ19 showed higher biodegradation ratios for steranes and hopanes

Tables 5–6 lists the numbers or/and abbreviation of the compounds identified in Figs 5–6.

3.3.1 Steranes

The distribution of C_{27}–C_{28}–C_{29} steranes can serve as an effective indicator to differentiate crude oils from different source rocks or organic facies of the same source rocks (Seifert and Moldowan, 1986; Peters et al., 2005). Biodegradation can affect thermal maturity parameters. For example, the preferential removal of 20R configurations results in an increased maturity index 20S/(20S + 20R). The results of the semiquantitative GC–MS analyses of steranes are shown in Table 5 and Fig 5. The total concentration of steranes in the presence of *P. aeruginosa* XJ16 decreased from 924.9 μg/g to 605.7 μg/g, equaling a total biodegradation ratio of 34.5%, and that in the presence of *A. lwoffi* XJ19 decreased from 924.9 μg/g to 479.4 μg/g, equaling a total biodegradation ratio of 48.2%, which was higher than that in the presence of *P.*

aeruginosa XJ16.

The diastrane biodegradation sequences were C_{29}diastrane (63.5%–76.7%) > C_{27}diastrane (26.9%–34.2%) for *P. aeruginosa* XJ16 and C_{29}diastrane (48.3%–78.9%) > C_{27}diastrane (-8.7%–42.5%) for *A. lwoffi* XJ19. Biodegradation results in the loss of selective configurations of βαC_{27}20S relative to βαC_{27}20R (Serfert and Moldowan, 1979). In this study, the biodegradation ratios of S-configuration diastranes were higher than those of R-configuration diastranes, being βαC_{27}20S(42.5%) > βαC_{27}20R(25.9%), αβC_{27}20S(29.5%) > αβC_{27}20R(−8.7%), and αβC_{29}20S (78.9%) > βαC_{29}20R (48.3%) for *A. lwoffi* XJ19 and βαC_{27}20S (32.0%) > βαC_{27}20R (27.5%) and αβC_{29}20S (76.7%) > βαC_{29}20R (63.5%) for *P. aeruginosa* XJ16 [except for αβC_{27}20S (26.8%) < αβC_{27}20R (34.2%) for *P. aeruginosa* XJ16]. The biodegradation sequences of pregnane and homopregnane were C_{22}-5α(H)-homopregnane (46.9%) > C_{21}-5α(H)-pregnane (32.2%) for *P. aeruginosa* XJ16 and C_{22}-5α(H)-homopregnane (45.4%) > C_{21}-5α(H)-pregnane (32.2%) for *A. lwoffi* XJ19.

In this study, the biodegradation sequence of αααC_{27}20R > αααC_{28}20R > αααC_{29}20R sterane was consistent with previous observations of removal in the order of αααC_{27}20R > αααC_{28}20R > αααC_{29}20R sterane (Peters et al., 1993; Chosson et al., 1992), indicating that αααC_{29}20R sterane shows higher bioresistance than αααC_{27}20R sterane (Peters et al., 2005). In general, sterane biodegradation occurs in the following sequence: ααα20R > αββ20R ≥ αββ20S ≥ ααα20S (Volkman et al., 1983), similarly, αααC_{27}20R (76.7%) > αββC_{27}20R (49.5%) ≥ αββC_{27}20S (48.8%) > αααC_{27}20S

(43.3%) occurs for *A. lwoffi* XJ19. The selective degradation of the natural R configurations over the geochemically formed S isomers has been confirmed by field observations (RullkÖtter and Wendisch, 1982; Serfert et al., 1984; Landeis and Connan, 1986), environmental studies of oil spills (Mille et al., 1998; Wan et al., 2001), and bacterial simulation experiments (Goodwin et al., 1983; Chosson et al., 1991; Díez et al., 2010). For *P. aeruginosa* XJ16, similar experimental results [αααC_{27}20R (63.6%) > αββC_{27}20R (39.3%), αααC_{27}20S (39.3%) > αββC_{27}20S (35.9%)] were obtained in this study, which was also consistent with previous observations of removal in the order of ααα20R > αββ20R > ααα20S > αββ20S for the epimers according to their susceptibilities to biodegradation (Seifert and Moldowan, 1979; McKirdy et al., 1983; Volkman et al., 1983; Connan, 1984; Peters et al., 2005). C_{28} steranes generally followed the order αααC_{28}20R (48.0%) > αααC_{28}20S (39.5%) > αββC_{28}20R (30.8%), αββC_{28}20S (28.1%) for *P. aeruginosa* XJ16 and αααC_{28}20R (59.9%) > αααC_{28}20S (51.6%) > αββC_{28}20S (44.5%), αββC_{28}20R (38.2%) for *A. lwoffi* XJ19. However, the S isomers of C_{29} steranes were more easily biodegraded in this study, being αααC_{29}20S (40.1%) > αββC_{29}20R (21.5%) > αββC_{29}20S (13.0%) > αααC_{29}20R (6.2%) for *P. aeruginosa* XJ16 and αααC_{29}20S (53.5%) > αββC_{29}20R (46.1%) > αββC_{29}20S (40.5%) > αααC_{29}20R (36.4%) for *A. lwoffi* XJ19.

3.3.2 Hopanes

Hopanes, a series of pentacyclic triterpanes derived from bacterial lipid precursors, are abundant in crude oil (Ourisson et al., 1979; Prince et al., 1993). Hopane

degradation under laboratory conditions has often been unsuccessful possibly because of the short time of incubation, use of pure cultures, absence of hopane-degrading bacteria, or inadequate conditions for growth (Connan et al., 1984; Rubinstein et al., 1977; Teschner et al., 1985; Prince et al., 1994). The results of the semiquantitative GC–MS analyses of hopanes are shown in Table 6 and Fig 6. The total concentration of the hopanes in the presence of *P. aeruginosa* XJ16 decreased from 2636.2 μg/g to 1997.1 μg/g, equaling a total biodegradation ratio of 24.2%, and that in the presence of *A. lwoffi* XJ19 decreased from 2636.2 μg/g to 1507.7 μg/g, equaling a total biodegradation ratio of 42.8%, which was higher than that in the presence of *P. aeruginosa* XJ16.

The biodegradation ratio of 17α(H),21β(H)-hopane ($C_{30}H$) was 21.9% for *P. aeruginosa* XJ16 and 46.9% for *A. lwoffi* XJ19. Hopane biodegradation has been associated with a proposed C-10 demethylation of the hopane A/B rings generating the corresponding 25-norhopanes (Peters et al., 1993, 1996; Reed et al., 1977; Seifert et al., 1979). In the present study, 25-norhopanes were not detected, which have been reported in naturally biodegraded crude oils (Peters et al., 1993; Seifert et al., 1979, 1984), suggesting an alternative mechanism of hopane biodegradation. However, in those cases, hopanes depletion was preceded by sterane biodegradation. Two separate hopane biodegradation pathways have been proposed: (1) demethylation of hopanes to 25-norhopanes prior to sterane degradation or (2) degradation of hopanes without 25-norhopane formation preceded by sterane degradation (Brooks et al., 1988).

The biodegradation of C_{31}–C_{35} homohopanes that occur as 22S and 22R epimers

400 based on the asymmetric center at C-22 (Peters et al., 1996), with a preferential
401 biodegradation of higher-molecular-weight homologues (C_{35} > C_{34}> C_{33}> C_{32}> C_{31}>
402 C_{30}), has been reported (Goodwin et al., 1983; Chosson et al., 1992). In this
403 mechanism, bacteria attack the homohopane molecule by oxidizing the side chain,
404 thus favoring higher-molecular-weight homologues (Moldowan et al., 1995). Other
405 studies have reported the preferential biodegradation of lower-molecular-weight
406 homohopanes, in which bacteria attack the cyclic core, resulting in the preferential
407 biodegradation of lower-molecular-weight homohopanes (Bost et al., 2001;
408 Moldowan et al., 1995). The biodegradation ratios of C_{31}, C_{32}, C_{33}, and C_{34}
409 homohopanes (22R) in the presence of *P. aeruginosa* XJ16 were 42.2%, 32.3%,
410 18.5%, and −16.1%, respectively, and the corresponding biodegradation ratios of C_{31},
411 C_{32}, C_{33}, and C_{34} homohopanes (22S) were 28.3%, 23.2%, −0.02%, and −11.4%,
412 respectively; therefore, the biodegradation sequence of C_{31}–C_{34} homohopanes was
413 C_{31} > C_{32} > C_{33} > C_{34}, and the biodegradation ratios of R-configuration homohopanes
414 were higher than those of S-configuration homohopanes (except for C_{34}
415 homohopanes). In the presence of *A. lwoffi* XJ19, the biodegradation ratios of C_{31}, C_{32},
416 C_{33}, and C_{34} homohopanes (22R) were 48.0%, 48.5%, 30.5%, and 0.23%, respectively,
417 and the corresponding biodegradation ratios of C_{31}, C_{32}, C_{33}, and C_{34} homohopanes
418 (22S) were 43.7%, 36.3%, 25.4%, and 24.5%, respectively; therefore, the
419 biodegradation sequence of C_{31}–C_{34} homohopanes was C_{31} > C_{32} > C_{33} > C_{34}, and the
420 biodegradation ratios of R-configuration homohopanes were higher than those of
421 S-configuration homohopanes (except for C_{34} homohopanes).

422 The Ts/(Ts + Tm) ratio has been used as a maturity index for source-related oils
423 because Tm is less thermally stable than Ts (Peters et al., 1993). The Ts/Tm ratio may
424 also change because of the relatively greater biodegradation ratio of Tm (Wang et al.,
425 1998; Peters et al., 1993). A Preferential biodegradation of Tm over Ts was observed,
426 being Tm (51.3%) > Ts (29.3%) for *P. aeruginosa* XJ16 and Tm (59.3%) > Ts (47.3%)
427 for *A. lwoffi* XJ19. The observed C_{29}M (57.8%) > C_{29}H (22.1%) and C_{30}M (30.0%) >
428 C_{30}H (21.9%) by *P. aeruginosa* XJ16 and C_{29}M (54.1%) > C_{29}H (42.9%) by *A. lwoffi*
429 XJ19 possibly contradict the preferential removal of αβ-hopanes relative to the
430 corresponding βα-moretanes during biodegradation (Pan et al., 2017). Similar
431 biodegradation ratios of C_{30}H (21.9%) and C_{29}H (22.1%) in the presence of *P.*
432 *aeruginosa* XJ16 as well as of C_{30}H (46.9%) and C_{29}H (42.9%) in the presence of *A.*
433 *lwoffi* XJ19 contradicted the preferential removal of the C_{30} αβ-hopane relative to its
434 C_{29} homologue (Peters et al., 2005). The biodegradation ratios of C_{30}* (39.1%) and
435 C_{29}Ts (30.6%) in the presence of *A. lwoffi* XJ19 were higher than those in the
436 presence of *P. aeruginosa* XJ16 (C_{30}*: 23.0%; C_{29}Ts: 7.47%). Both *P. aeruginosa*
437 XJ16 (70.8%) and *A. lwoffi* XJ19 (63.3%) showed the highest biodegradation ratio for
438 18α(H)-oleanane of the hopane series.

439 3.4 Different biodegradation sequences of compounds

440 Although crude oil biodegradation is often explained as a quasi-stepwise process in
441 which various components are removed in a well-recognized sequence (*n*-alkanes >
442 *n*-alkylcyclohexanes > acyclic isoprenoids > bicyclic sesquiterpenes > steranes >

443 hopanes) (George et al., 2002), bacteria do not biodegrade compounds in a stepwise
444 manner. Rather, they utilize different compounds simultaneously at different rates. For
445 *P. aeruginosa* XJ16 (Fig. 7), the general biodegradation sequence of compounds was
446 *n*-alkanes (most easily to biodegrade) > *n*-alkylcyclohexanes > dicyclic
447 sesquiterpenes > steranes > hopanes (most difficult to biodegrade). In general,
448 *n*-alkanes are among the first hydrocarbons to be removed (Greenwood et al., 2008).
449 However, for *A. lwoffi* XJ19 (Fig. 7), the general biodegradation sequence of
450 compounds was dicyclic sesquiterpenes (most easily to biodegrade) > steranes >
451 hopanes > *n*-alkylcyclohexanes > *n*-alkanes (most difficult to biodegrade). The
452 biodegradability of *n*-alkanes, *n*-alkylcyclohexanes, and dicyclic sesquiterpenes in the
453 presence of *P. aeruginosa* XJ16 was higher than that in the presence of *A. lwoffi* XJ19
454 (Fig. 7). However, the biodegradability of steranes and hopanes in the presence of *A.*
455 *lwoffi* XJ19 was higher than that in the presence of *P. aeruginosa* XJ16 (Fig. 7). For *A.*
456 *lwoffi* XJ19, whether it has only completed the initial biodegradation but not the
457 complete biodegradation needs further simulation experiments to study.

458 **4. Conclusions**

459 The saturated hydrocarbon biomarkers were actually destroyed simultaneously but
460 at different ratios:

461 (1) *n*-alkanes: although both the bacterial strains could biodegrade C_{14}–C_{35}
462 *n*-alkanes, their total biodegradation ratio was higher in the presence of *P. aeruginosa*
463 XJ16 (98.8%) than in the presence of *A. lwoffi* XJ19 (29.3%). In the presence of *P.*

aeruginosa XJ16, the biodegradation ratios of relatively short-chain *n*-alkanes were higher than those of relatively long-chain *n*-alkanes (nC_{14}, nC_{15}, nC_{16}–nC_{26}, nC_{27}–nC_{28} > nC_{29}–nC_{32} > nC_{33} > nC_{34}–nC_{35}); however, in the presence of *A. lwoffi* XJ19, the biodegradation ratios of relatively long-chain *n*-alkanes were higher than those of relatively short-chain *n*-alkanes (nC_{14} > nC_{32}–nC_{33} > nC_{34}–nC_{35} > nC_{15}, nC_{29}–nC_{31} > nC_{27}–nC_{28} > nC_{16}–nC_{26}), indicating that the *n*-alkane biodegradation sequences for *P. aeruginosa* XJ16 and *A. lwoffi* XJ19 were different.

(2) *n*-alkylcyclohexanes: although both the bacterial strains could biodegrade C_8–C_{31} *n*-alkylcyclohexanes, their total biodegradation ratio was higher in the presence of *P. aeruginosa* XJ16 (97.1%) than in the presence of *A. lwoffi* XJ19 (44.3%). In the presence of *P. aeruginosa* XJ16, the biodegradation ratios of *n*-alkylcyclohexanes, except nC_8-cHex, were greater than 85% (nC_9–nC_{25}-cHex, nC_{26}–nC_{28}-cHex, nC_{29}–nC_{31}-cHex>nC_8-cHex). However, in the presence of *A. lwoffi* XJ19, the biodegradation ratios of relatively long-chain *n*-alkylcyclohexanes were higher than those of relatively short-chain *n*-alkylcyclohexanes (nC_{31}–nC_{29}-cHex> nC_{28}–nC_{26}-cHex>nC_{25}–nC_9-cHex>nC_8-cHex), indicating that the *n*-alkylcyclohexane biodegradation sequences for *P. aeruginosa* XJ16 and *A. lwoffi* XJ19 were different.

(3) Bicyclic sesquiterpenes: although the total biodegradation ratios were higher in the presence of *P. aeruginosa* XJ16 (74.9%) than in the presence of *A. lwoffi* XJ19 (58.5%), the biodegradation sequences for *P. aeruginosa* and *A. lwoffi* XJ19 were the same (C_{14}-bicyclic sesquiterpene > C_{15}-bicyclic sesquiterpene > 8α(H)-drimane, 8β(H)-drimane > C_{15}-bicyclic sesquiterpene, C_{16}-bicyclic sesquiterpene,

8β(H)-homodrimane).

(4) Steranes: the total biodegradation ratios were higher in the presence of *A. lwoffi* XJ19 (48.2%) than in the presence of *P. aeruginosa* XJ16 (34.5%). Except for the similar biodegradation ratios of pregnane and homopregnane in the presence of these bacteria, the biodegradation ratios of other steranes were slightly higher in the presence of *A. lwoffi* XJ19 than in the presence of *P. aeruginosa* XJ16. The sterane biodegradation sequences for these bacteria were similar: C_{29}diastrane > C_{27}diastrane, C_{22}-5α(H)-homopregnane > C_{21}-5α(H)-pregnane, βαC_{27}20S > βαC_{27}20R, αβC_{27}20S > αβC_{27}20R, and αααC_{27}20R > αααC_{28}20R > αααC_{29}20R.

(5) Hopanes: the total biodegradation ratio were higher in the presence of *A. lwoffi* XJ19 (42.8%) than in the presence of *P. aeruginosa* XJ16 (24.2%). The biodegradation ratios of hopanes were higher in the presence of *A. lwoffi* XJ19 than in the presence of *P. aeruginosa* XJ16 [except for 17β(H),21α(H)-30 normoretane, 18α(H)-oleanane and 17β(H),21α(H)-30 homomoretane (22S + 22R)]. Depletion of the C_{31}–C_{34} homohopanes was also observed, with a preferential biodegradation of lower-molecular-weight homologues (C_{31} > C_{32} > C_{33} > C_{34}) and R epimer over S epimer. The hopane biodegradation sequences for *P. aeruginosa* XJ16 and *A. lwoffi* XJ19 were similar: Tm > Ts, C_{29}M > C_{29}H, and C_{30}H = C_{29}H.

Therefore, the general biodegradation sequences of compounds in saturated hydrocarbons for *P. aeruginosa* XJ16 (*n*-alkanes > *n*-alkylcyclohexanes > dicyclic sesquiterpenes > steranes > hopanes) and *A. lwoffi* XJ19 (dicyclic sesquiterpenes > steranes > hopanes > *n*-alkylcyclohexanes > *n*-alkanes) are different, thus proving the

effects of different bacterial species on crude oil biodegradation.

Acknowledgments

This study was financially supported by National Science and Technology Major Project (2016ZX05050011, 2016ZX05040002), and National Natural Science Foundation of China (41373086). We thank the PetroChina Changqing Oilfield Company for their assistance with sampling. We are also thankful to Xiaoli Liu, ShengBao Shi, and Lei Zhu of the China University of Petroleum (Beijing) for their help with the experiments. All data presented in the manuscript are listed in the tables.

References

Agyingi, C.M., Abanda, P.A., Fozao, K.F., Njoha, O.A., Epantya, A.F., Tangkoa, N.C., Kwangkama, F.N., and Esemec E., 2019. Geochemistry of Seep and Produced Oil Samples from Southern Cameroon. Journal of Petroleum Geology 42(2): 193–206.

Alberdi, M., Moldowan, J.M., Peters, K.E., Dahl, J.E., 2001 Stereoselective biodegradation of tricyclic terpanes in heavy oils from the Bolivar Coastal Fields, Venezuela. Organic Geochemistry 32: 181–191.

Alon, R.N., Gutnick, D.L., 1993. Esterase from the oil-degrading *Acinetobacter lwoffii* RAG-1: sequence analysis and over-expression in escherichia coli. Fems Microbiology Letters 112(3), 275–280.

Amund, O.O., and I.J. Higgins., 1985. The degradation of 1-phenylalkanes by an oil-degrading strain of *Acinetobacter lwoffii*. Antonie Leeuwenhoek 51, 45–56.

528 Andrew, S. R., Paul, F., Michael E., Steve, R. L., 2010. Geochemical compositional
529 gradients in a mixed oil reservoir indicative of ongoing biodegradation. Organic
530 Geochemistry 41(3), 307-320.
531 Aparna, A., Srinikethan, G., Smitha, H., 2012. Production and characterization of
532 biosurfactant produced by a novel Pseudomonas sp. 2B. Colloids Surf B
533 Biointerfaces 95, 23-29.
534 Beam, H.W., and J.J. Perry., 1974. Microbial degradation and assimilation of
535 *n*-alkyl-substituted cycloparaffins. Journal of Bacteriology 118, 394–399.
536 Bicalho, B., Chen, L.S., Grognux, J., Reymond, J.L., Marsaioli, A.J., 2004. Studies on
537 whole cell fluorescence-based screening for epoxide hydrolases and
538 Baeyer-Villiger monoxygenases. Journal of the Brazilian Chemical Society 15,
539 911–916.
540 Bost, F.D., Frontera-Suau, R., McDonald, T.J., Peters, K.E., Morris, P.J., 2001.
541 Aerobic biodegradation of hopanes and norhopanes in Venezuelan crude oils.
542 Organic Geochemistry 32, 105–114.
543 Brooks, P.W., Fowler, M.G., Macqueen, R.W., 1988. Biological marker and
544 conventional organic geochemistry of oil sands/heavy oils, Western Canada Basin.
545 Organic Geochemistry 12, 519–538.
546 Cheng, X., Hou, D., Xu, C., Wang, F., 2016. Biodegradation of tricyclic terpanes in
547 crude oils from the bohai bay basin. Organic Geochemistry 101, 11–21.
548 Chosson, P., Lanau, C., Connan, J., Dessort, D., 1991. Biodegradation of refractory
549 hydrocarbon biomarkers from petroleum under laboratory conditions. Nature 351,

640–642.

Chosson, P., Connan, J., Dessort, D., Lanau, C., 1992. In vitro biodegradation of steranes and terpanes: a clue to understanding geological situations. In Biological Markers in Sediments and Petroleum (Moldowan, J.M., Albrecht, P., Philp, R.P. (Eds.)). Prentice-Hall, Englewood Cliffs, NJ, pp. 320–349.

Connan, J., 1984. Biodegradation of crude oils in reservoirs. In: Brooks, J., Welte, D.H. (Eds.), Advances in Petroleum Geochemistry I. Academic Press, London, pp. 298–335.

Díez, S., Sabatté, J., Viñas, M., Bayona, J.M., Solanas, A.M., Albaigés, J., 2010. The prestige oil spill. I. Biodegradation of a heavy fuel oil under simulated conditions. Environmental Toxicology & Chemistry 24(9), 2203–2217.

Du, W.D., Wan, Y.Y., Zhong, N.N., Fei, J.J., Zhang, Z.H., Chen, L.J., Hao, J.M., 2011. Status quo of soil petroleum contamination and evolution of bioremediation. Petroleum Science 8(4), 502–514.

Essaid, H.I., Bekins, B.A., Godsy, E.M., Warren, E., Baedecker, M.J., Cozzarelli, I. M., 1995. Simulation of aerobic and anaerobic biodegradation processes at a crude oil spill site. Water Resources Research 31(12), 3309–3327.

Frances, D.H., Keith, A.K., 2002. Alkvlcvclohexanes in Environmental Geochemistry. Environmental Forensics 3, 293–301.

George, S.C., Boreham, C.J., Minifie, S.A., Teerman, S.C., 2002. The effect of minor to moderate biodegradation on C_5 to C_9 hydrocarbons in crude oils. Organic Geochemistry 33(12), 1293–1317.

572 Goodwin, N.S., Park, P.J.D., Rawlinson, T., 1983. Crude oil biodegradation under
573 simulated and natural conditions. In: Bjorøy, M. et al. (Eds.), Advances in Organic
574 Geochemistry 1981. Wiley, Chichester, pp. 650–658.
575 Goswami, P., Singh, H.D., 1991. Different modes of hydrocarbon uptake by two
576 *Pseudomonas species*. Biotechnology & Bioengineering 37 (1), 1–11.
577 Greenwood, A.F., Wibrow, S., George, S.J., Tibbett, M., 2008. Sequential
578 hydrocarbon biodegradation in a soil from arid coastal australia, treated with oil
579 under laboratory controlled conditions. Organic Geochemistry 39(9), 1336–1346.
580 Head, I.M., Jones, D.M., Larter, S.R., 2003. Biological activity in the deep subsurface
581 and the origin of heavy oil. Nature 426: 344–352.
582 Huang, H.P., Li, J., 2017. Molecular composition assessment of biodegradation
583 influence at extreme levels – a case study from oilsand bitumen in the Junggar
584 basin, NW China. Organic Geochemistry 103, 31–42.
585 Jones, D.M., Head, I.M., Gray, N.D., Adams, J.J., Rowan, A.K., Aitken, C.M.,
586 Bennett, B., Huang, H., Brown, A., Bowler, B.F.J., Oldenburg, T., Erdmann, M.,
587 Larter, S. R. 2008. Crude-oil biodegradation via methanogenesis in subsurface
588 petroleum reservoirs. Nature 451, 176–180.
589 Kaplan, I.R., Galperin, Y., Lu, S.T., Lee, R.P., 1997. Forensic environmental
590 geochemistry: Differentiation of fuel types, their sources, and release time. Organic
591 Geochemistry 27, 289–317.
592 Koma, D., Hasumi, F., Chung, S.Y., Kubo, M., 2003. Biodegradation of
593 *n*-Alkylcyclohexanes by Co-Oxidation via Multiple Pathways in *Acinetobacter* sp.

ODDK71. Journal of Bioscience and Bioengineering 95(6), 641–644.

Koopmans, M. P., Larter, S.R., Zhang, C., Mei, B., Wu, T., Chen, Y., 2002. Biodegradation and mixing of crude oils in Eocene Es3 reservoirs of the Liaohe Basin, northeastern China. American Association of Petroleum Geologists Bulletin 86 (10), 1833–1843.

Landais, P., Connan, J., 1986. Source rock potential and oil alteration in the uraniferous basin of Lodève (Hérault, France). Sciences Géologiques Bulletin 39 (3), 468–476.

Larter, S.R., Wilhelms, A., Head, I.M., Koopmans, M., Aplin, A., di Primio, R., Zwach, Z., Erdmann, M., Telnaes, N., 2003. The controls on the composition of biodegraded oils in the deep subsurface – Part 1: biodegradation rates in petroleum reservoirs. Organic Geochemistry 34, 601–613.

Larter, S.R., Huang, H., Adams, J.J., Bennett, B., Jokanola, O., Oldenburg, T.B.P., Jones, M., Head, I., Riediger, C.L., Fowler, M.G., 2006. The controls on the composition of biodegraded oils in the deep subsurface. Part II – geological controls on subsurface biodegradation fluxes and constraints on reservoir-fluid property prediction. American Association of Petroleum Geologists Bulletin 90, 921–938.

Liao, Y., Shi, Q., Hsu, C.S., Pan, Y., Zhang, Y., 2012. Distribution of acids and nitrogen-containing compounds in biodegraded oils of the liaohe basin by negative ion ESI FT-ICR MS. Organic Geochemistry 47(6), 51–65.

Lin, L.H., Michael G.E., Kovachev, G., Zhu, H., Philp, R.P., Lewis, C.A., 1989.

Biodegradation of tar-sand bitumens from the Ardmore and Anadarko Basins, Carter County, Oklahoma. Organic Geochemistry. 14: 511–523.

Liu, H., Liang, R., Tao, F., Ma, C., Liu, Y., Liu, X.P., Liu, J.H., 2012. Genome sequence of *Pseudomonas aeruginosa* strain SJTD-1, a bacterium capable of degrading longchain alkanes and crude oil. J. Bacteriol 194, 4783–4784. Journal of Bacteriology

McKirdy, D.M., Aldridge, A.K., Ypma, P.J.M., 1983. A geochemical comparison of some crude oils from pre-Ordovician carbonate rocks. In: Bjorøy, M. et al. (Eds.), Advances in Organic Geochemistry 1981. Wiley, Chichester, pp. 99–107.

Meredith, W., Kelland, S.J., Jones, D.M., 2000. Influence of biodegradation on crude oil acidity and carboxylic acid composition. Organic Geochemistry. 31: 1059–1073.

Mille, G., Munoz, D., Jacquot, F., Rivet, L., Bertrand, J.C., 1998. The amoco cadiz oil spill: evolution of petroleum hydrocarbons in the ile grande salt marshes (brittany) after a 13-year period. Estuarine Coastal & Shelf Science 47(5), 547–559.

Mishra, S., Panda, S., Pradhan, N., Satapathy, D., Biswal, S.K., Mishra, B.K., 2017. Insights into DBT biodegradation by a native *Rhodococcus* strain and its sulphur removal efficacy for two indian coals and calcined pet coke. International Biodeterioration & Biodegradation 120, 124–134.

Mnif, Inès, Elleuch, M., Chaabouni, S.E., Ghribi, D., 2013. Bacillus subtilis SPB1 biosurfactant: production optimization and insecticidal activity against the carob moth ectomyelois ceratoniae. Crop Protection 50, 66-72.

Moldowan, J.M., McCaffrey, M.A., 1995. A novel microbial hydrocarbon degradation

638 pathway revealed by hopane demethylation in a petroleum reservoir. Geochimica et
639 Cosmochimica Acta 59, 1891–1894.
640 Oblasov, N.V., Goncharov, I.V., Samoilenko, V.V., Van Graas, G. W., 2018.
641 Biodegradation in the Nkh 3-4 reservoir at vankor field (west siberia basin, russia)
642 is strongly controlled by rock properties. Organic Geochemistry,
643 S014663801830024X.
644 Oldenburg, T.B.P., Jones, M., Huang, H.P., Bennett, B., Shafiee, N. S., Head, I., Steve
645 R. L., 2017. The controls on the composition of biodegraded oils in the deep
646 subsurface-part 4. destruction and production of high molecular weight
647 non-hydrocarbon species and destruction of aromatic hydrocarbons during
648 progressive in-reservoir biodegradation. Organic Geochemistry, 114: 57–80.
649 Ourisson, G., Albrecht, P., Rohmer, M., 1979. The hopanoids. Palaeochemistry and
650 biochemistry of a group ofnatural products. Pure and Applied Chemistry 51,
651 709–729.
652 Pan, Y.H., 2015. The Study on the Effect of Biodegradation on the Chemical
653 Compositions of Liaohe Crude Oils (Ph.D. thesis). Guangzhou: Guangzhou
654 Institute of Geochemistry, Chinese Academy of Sciences.
655 Pan, Y.H, Liao. Y., Shi. Q, 2017. Variations of Acidic Compounds in Crude Oil during
656 Simulated Aerobic Biodegradation: Monitored by Semiquantitative Negative-Ion
657 ESI FT-ICR MS. Energy & Fuels 31, 1126–1135.
658 Peters, K.E., Moldowan, J.M., 1993. The Biomarker Guide: Interpreting Molecular
659 Fossils in Petroleum and Ancient Sediments. Prentice Hall, Englewood Cliffs, NJ,

660 USA.
661 Peters, K.E., Moldowan, J.M., McCaffrey, M.A., Fago, F.J., 1996. Selective
662 biodegradation of extended hopanes to 25-norhopanes in petroleum reservoirs.
663 Insights from molecular mechanics. Organic Geochemistry 24, 765–783.
664 Peters, K.E., Walters, C.C., Moldowan, J.M., 2005. The Biomarker Guide,
665 Biomarkers and Isotopes in Petroleum Exploration and Earth History. Cambridge
666 University Press, New York.
667 Prince, R.C., 1993. Petroleum spill bioremediation in marine environments. Critical
668 Reviews in Microbiology 19(4), 217–240.
669 Prince, R.C., Elmendorf, D.L., Lute, J.R., Hsu, C.S., Halth, C.E., Sensius, J.D.,
670 Dechert, G.J., Douglas, G.S., Butler, E.L., 1994. 17α(H), 21β(H)-hopane as a
671 conserved internal standard for estimating the biodegradation of crude oil.
672 Enironmental Science &Technology 28, 142–145.
673 Reed, W.E., 1977. Molecular compositions of weathered petroleum and comparison
674 with its possible source. Geochimica et Cosmochimica Acta 41, 237–247.
675 Roling, W.F.M., Head, I.M., Larter, S.R., 2003. The microbiology of hydrocarbon
676 degradation in subsurface petroleum reservoirs: perspectives and prospects.
677 Research in Microbiology. 154(5): 321–328.
678 Rubinstein, I., Strausz, O.P., Spyckerelle, C., Crawford, R.J., Westlake, D.W.S., 1977.
679 The origin of oil sandbitumens of Alberta. Geochimica et Cosmochimica Acta 41,
680 1341–1353.
681 Rullkötter, J., Wendisch, D., 1982. Microbial alteration of 17α(H)-hopanes in

682 Madagascar asphalts: removal of C-10 methyl group and ring opening. Geochimica
683 et Cosmochimica Acta 43, 1545–1554.
684 Seifert, W.K., Moldowan, J.M., 1979. The effect of biodegradation on steranes and
685 terpanes in crude oils. Geochimica et Cosmochimica Acta 43, 111–126.
686 Seifert, W.K., Moldowan, J.M., Demaison, G.J., 1984. Source correlation of
687 biodegraded oils. Organic Geochemistry 6, 633–643.
688 Seifert, W.K., Moldowan, J.M., 1986. Use of biological markers in petroleum
689 exploration. In: Johns, R.B. (Ed.), Biological Markers in the Sedimentary Record
690 24, Methods in Geochemistry and Geophysics. Elsevier, pp. 261–290.
691 Teschner, M. and Wehner, H., 1985. Chromatographic investigations of biodegraded
692 crude oils. Chromatographia 20, 407–416.
693 Throne-Holst, M., Wentzel, A., Ellingsen, T.E., Kotlar, H.K., Zotchev, S.B., 2007.
694 Identification of novel genes involved in long-chain *n*-alkane degradation by
695 *Acinetobacter* sp. strain DSM 17874. Applied and Environmental Microbiology
696 73(10), 3327–3332.
697 Trudgill, P.W., 1984. Microbial degradation of the alicyclic ring: structural
698 relationship and metabolic pathways, p. 131–180. In D. T. Gibson (ed.), Microbial
699 degradation of organic compounds. Marcel Dekker, New York, N.Y.
700 Varjani, S.J., Upasani, V.N., 2016. Biodegradation of petroleum hydrocarbons by
701 oleophilic strain of *Pseudomonas aeruginosa* NCIM 5514. Bioresource Technology
702 222, 195–201.
703 Varjani, S.J., Gnansounou, E., 2017. Microbial dynamics in petroleum oilfields and

704 their relationship with physiological properties of petroleum oil reservoirs.
705 Bioresource Technology, 245(Pt A).
706 Volkman, J.K., Alexander, R., Kagi, R.I., Woodhouse, G.W., 1983. Demethylated
707 hopanes in crude oils and their applications in petroleum geochemistry. Geochimica
708 et Cosmochimica Acta 47, 785–794.
709 Volkman, J.K., Alexander, R., Kagi, R.I., Rowland, S.J., Sheppard, P.N., 1984.
710 Biodegradation of aromatic hydrocarbons in crude oils from the barrow sub-basin
711 of western australia. Organic Geochemistry 6, 619–632.
712 Wan, Z., Fingas, M., Owens, E.H., Sigouin, L., Brown, C.E., 2001. Long-term fate
713 and persistence of the spilled metula oil in a marine salt marsh environment
714 degradation of petroleum biomarkers. Journal of Chromatography A 926(2),
715 275–290.
716 Wang, Z.D., Fingas, M., Blenkinsopp, S., Sergy, G., Landriault, M., Sigouin, L., Foght,
717 J., Semple, K., Westlake, D.W.S., 1998. Comparison of oil composition changes
718 due to biodegradation and physical weathering in different oils. Journal of
719 Chromatography A 809, 89–107.
720 Wenger, L.M., Davis, C.L., Isaksen, G.H., 2002. Multiple controls on petroleum
721 biodegradation and impact on oil quality. SPE Reservoir Evaluation & Engineering.
722 5: 375–383.
723 Williams, J.A., Bjorøy, M., Dolcater, D.L., Winters, J.C., 1986. Biodegradation in
724 south texas eocene oils-effects on aromatics and biomarkers. Organic Geochemistry
725 10(1), 451–461.

Yoshizako, F., Chubachi, M., Nishimura, A., Ueno, T., 1989. Metabolism of *n*-Alkylcyclohexanes with an Even Number of Carbon Atoms in the Side Chain by *Micrococcus* sp. RCO-4M. Journal of Fermentation and Bioengineering 67(5), 335–338.

Figs

Fig. 1. Sample before biodegradation and TIC of the saturated hydrocarbons of crude oil sample from the Changqing oilfield—the carbon source used in the aerobic biodegradation simulations **(a)**—the bacteria used in the biodegradation simulations; cell morphologies of *Pseudomonas aeruginosa* XJ16 **(b)** and *Acinetobacter lwoffii* XJ19 **(c)**; samples in biodegradation process and TIC of the saturated hydrocarbons of biodegraded crude oil. **Note**: nC_{17} = C_{17} *n*-alkane, nC_{18} = C_{18} *n*-alkane, Pr = Pristane and Ph = Phytane; Pa-10, Pa-20, Pa-40, Pa-60 and Pa-90 represent biodegraded oil by *P. aeruginosa* XJ16 **(d, f, h, j, l)** and Al-10, Al-20, Al-40, Al-60 and Al-90 represent biodegraded oil by *A. lwoffii* XJ19 **(e, g, i, k, m)** on day 10, 20, 40, 60 and 90, respectively.

Fig. 2. Total concentration (μg/g) of *n*-alkanes during biodegradation by *P. aeruginosa* XJ16 **(a)** and *A. lwoffii* XJ19 **(b)** (mean of three replicates; error bars represent averaged squared deviation). **Note**: nC_{14} ~ nC_{35} represent C_{14} *n*-alkane ~ C_{35} *n*-alkane of corresponding carbon number, respectively.

Fig. 3. Total concentration (μg/g) of *n*-alkylcyclohexanes during biodegradation by *P. aeruginosa* XJ16 **(a)** and *A. lwoffii* XJ19 **(b)** (mean of three replicates; error bars represent averaged squared deviation). **Note**: nC_8-cHex ~ nC_{31}-cHex represent C_8 *n*-alkylcyclohexane ~ C_{31} *n*-alkylcyclohexane of corresponding carbon number, respectively.

Fig. 4. Total concentration (μg/g) of bicyclic sesquiterpenes during biodegradation by *P. aeruginosa* XJ16 **(a)** and *A. lwoffii* XJ19 **(b)** (mean of three replicates; error bars represent averaged squared deviation). **Numbers** on the X-axis: 1: C_{14}-bicyclic sesquiterpene; 2: C_{14}-bicyclic sesquiterpene; 3: C_{15}-bicyclic sesquiterpene; 4: C_{15}-bicyclic sesquiterpene; 5:

8α(H)-drimane; 6: 8β(H)-drimane; 7: C_{15}-bicyclic sesquiterpene; 8: C_{16}-bicyclic sesquiterpene; 9: C_{15}-bicyclic sesquiterpene; 10: C_{16}-bicyclic sesquiterpene; 11: 8β(H)-homodrimane.

Fig. 5. Total concentration (μg/g) of steranes during biodegradation by *P. aeruginosa* XJ16 **(a)** and *A. lwoffii* XJ19 **(b)** (mean of three replicates; error bars represent averaged squared deviation). **Numbers** on the X-axis: 1: C_{21}-5α(H)-pregnane; 2: C_{22}-5α(H)-homopregnane; 3: βαC_{27}20S: 13β(H),17α(H)-C_{27}diastrane (20S); 4: βαC_{27}20R: 13β(H),17α(H)-C_{27}diastrane (20R); 5: αβC_{27}20S: 13α(H),17β(H)-C_{27}diastrane (20S); 6: αβC_{27}20R: 13α(H),17β(H)-C_{27}diastrane (20R); 7: αααC_{27}20S: 5α(H),14α(H),17α(H)-sterane (20S); 8: αββC_{27}20R: 5α(H),14β(H),17β(H)-sterane (20R); 9: αββC_{27}20S: 5α(H),14β(H),17β(H)-sterane (20S); 10: αααC_{27}20R: 5α(H),14α(H),17α(H)-sterane (20R); 11: βαC_{29}20R: 13β(H),17α(H)-C_{29}diastrane (20R); 12: αβC_{29}20S: 13α(H),17β(H)-C_{29}diastrane (20S); 13: αααC_{28}20S: 24-methyl-5α(H),14α(H),17α(H)-sterane (20S); 14: αββC_{28}20R: 24-methyl-5α(H),14β(H),17β(H)-sterane (20R); 15: αββC_{28}20S: 24-methyl-5α(H),14β(H),17β(H)-sterane (20S); 16: αααC_{28}20R: 24-methyl-5α(H),14α(H),17α(H)-sterane (20R); 17: αααC_{29}20S: 24-ethyl-5α(H),14α(H),17α(H)-sterane (20S); 18: αββC_{29}20R: 24-ethyl-5α(H),14β(H),17β(H)-sterane (20R); 19: αββC_{29}20S: 24-ethyl-5α(H),14β(H),17β(H)-sterane (20S); 20: αααC_{29}20R: 24-ethyl-5α(H),14α(H),17α(H)-sterane (20R)

Fig. 6. Total concentration (μg/g) of hopanes during biodegradation by *P. aeruginosa* XJ16 **(a)** and *A. lwoffii* XJ19 **(b)** (mean of three replicates; error bars represent averaged squared deviation). **Numbers** on the X-axis: 1: Ts: 18α(H)-22,29,30-trisnorneohopane; 2: Tm: 17α(H)-22,29,30-trisnorhopane; 3: C_{29}H: 17α,21β(H)-30 norhopane; 4: C_{29}Ts: 18α,21β(H)-30 norneohopane; 5: C_{30}*: C_{30} diahopane; 6: C_{29}M: 17β(H),21α(H)-30 normoretane; 7: Ol: 18α(H)-oleanane; 8: C_{30}H: 17α(H),21β(H)-hopane; 9: C_{30}M: 17β(H),21α(H)-moretane; 10: C_{31}H22S: 17α(H),21β(H)-30 homohopane(22S); 11: C_{31}H22R: 17α(H),21β(H)-30 homohopane(22R); 12: Gam: Gammacerane; 13: 17β(H),21α(H)-30 homomoretane(22S+22R); 14: C_{32}H22S: 17α(H),21β(H)-30,31 dihomohopane(22S); 15: C_{32}H22R: 17α(H),21β(H)-30,31 dihomohopane(22R); 16: C_{33}H22S: 17α(H),21β(H)-30,31,32 trihomohopane(22S); 17: C_{33}H22R:17α(H),21β(H)-30,31,32trihomohopane(22R); 18: C_{34}H22S:

17α(H),21β(H)-30,31,32,33 tetrahomohopane(22S); 19: C_{34}H22R: 17α(H),21β(H)-30,31,32,33 tetrahomohopane(22R); 20: C_{35}H22S: 17α(H),21β(H)-30,31,32,33,34 pentahomohopane(22S); 21: C_{35}H22R: 17α(H),21β(H)-30,31,32,33,34 pentahomohopane(22R)

Fig. 7. *P. aeruginosa* XJ16 and *A. lwoffii* XJ19 have the different biodegradation sequence of saturated hydrocarbon compounds. For each compound series, they have the different biodegradation sequence for *n*-alkanes and *n*-alkylcyclohexanes, but have the same biodegradation sequence for biomarkers of bicyclic sesquiterpenes, steranes and hopanes.

Tables

Table 1. Change of the biodegradation ratio (%) and four fractions (%) during biodegradation

Table 2. Removal of *n*-alkanes via biodegradation by *P. aeruginosa* XJ16 and *A. lwoffii* XJ19

Table 3. Removal of *n*-alkylcyclohexanes via biodegradation by *P. aeruginosa* XJ16 and *A. lwoffii* XJ19

Table 4. Removal of bicyclic sesquiterpenes via biodegradation by *P. aeruginosa* XJ16 and *A. lwoffii* XJ19

Table 5. Removal of steranes via biodegradation by *P. aeruginosa* XJ16 and *A. lwoffii* XJ19

Table 6. Removal of hopanes via biodegradation by *P. aeruginosa* XJ16 and *A. lwoffii* XJ19

Figure 1.

(a)crude oil

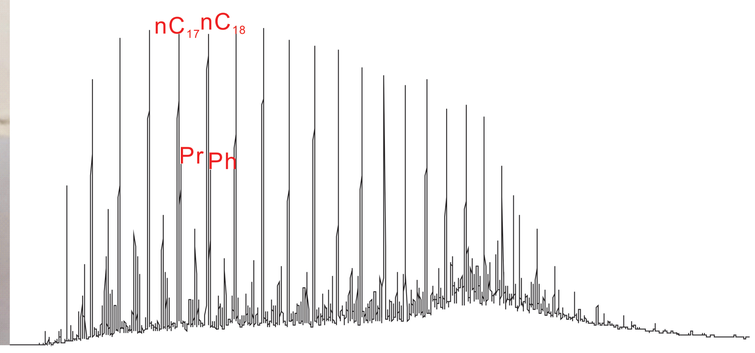

(b)*Pseudomonas aeruginosa* XJ16

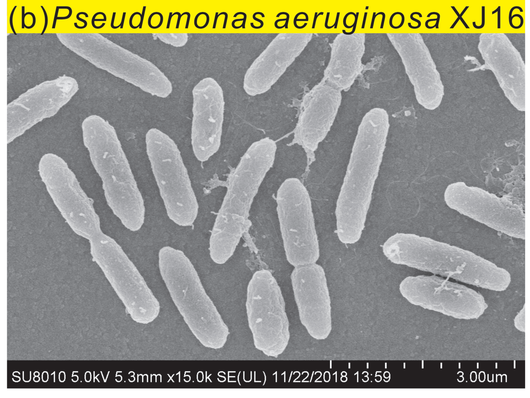

(c)*Acinetobacter lwoffii* XJ19

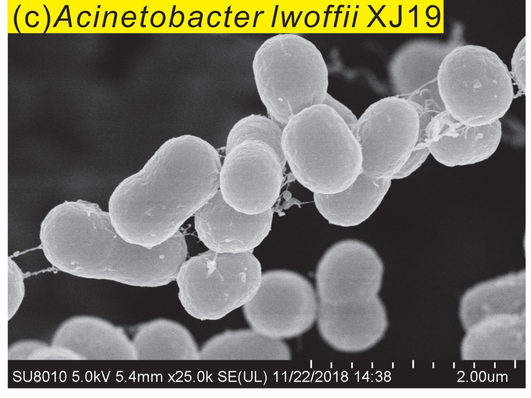

(d)Pa-10

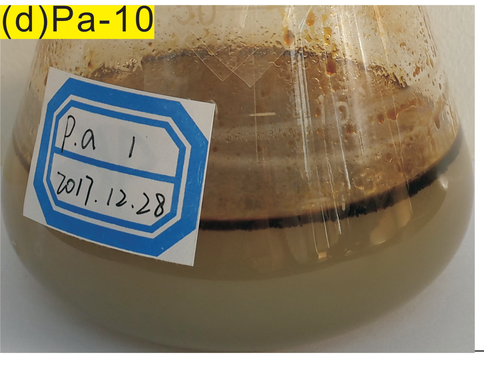

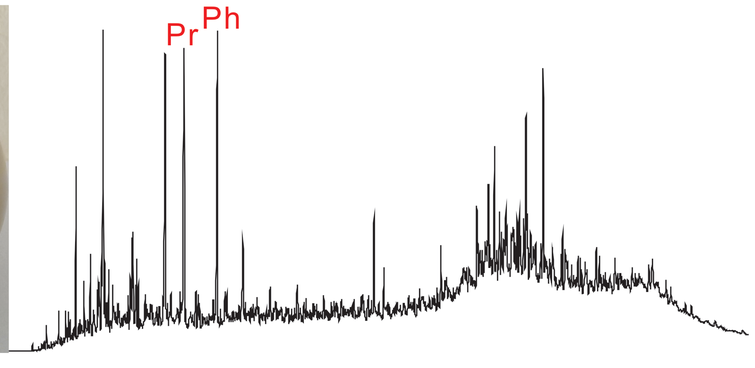

(e)Al-10

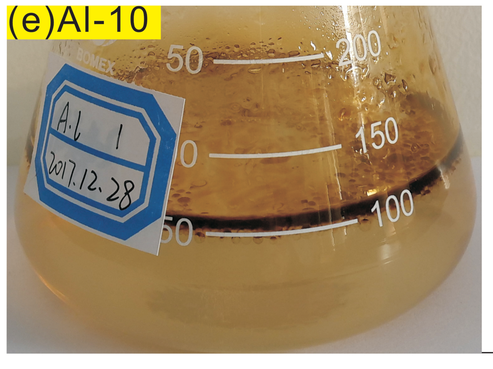

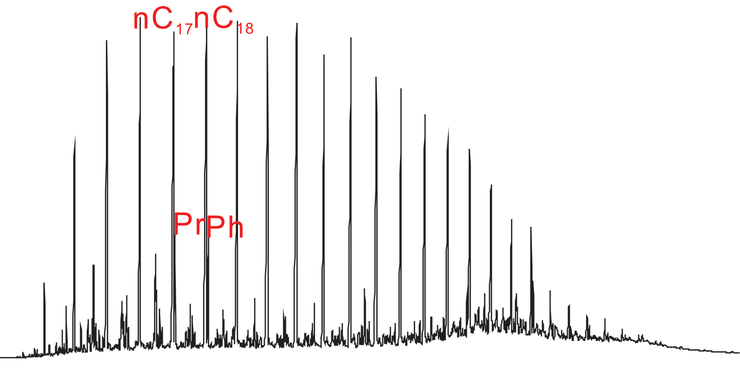

(f)Pa-20

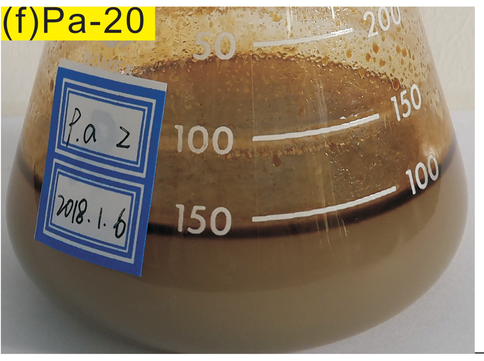

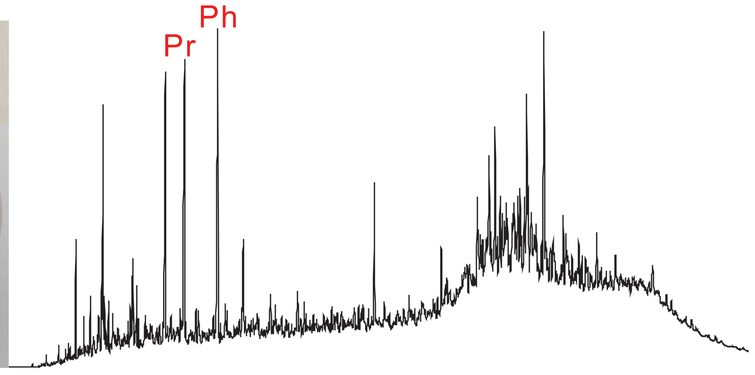

(g)Al-20

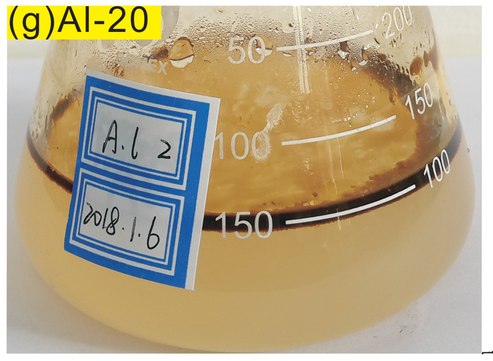

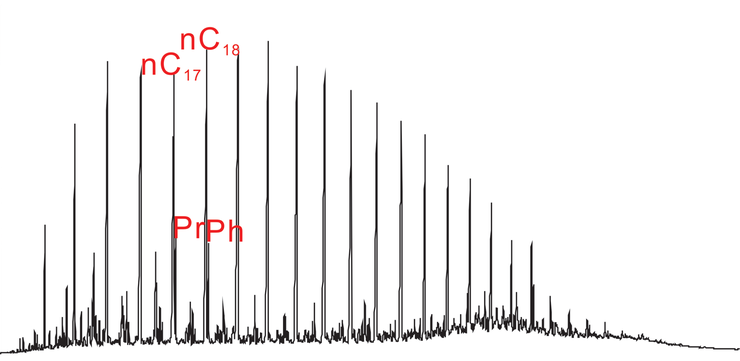

(h)Pa-40

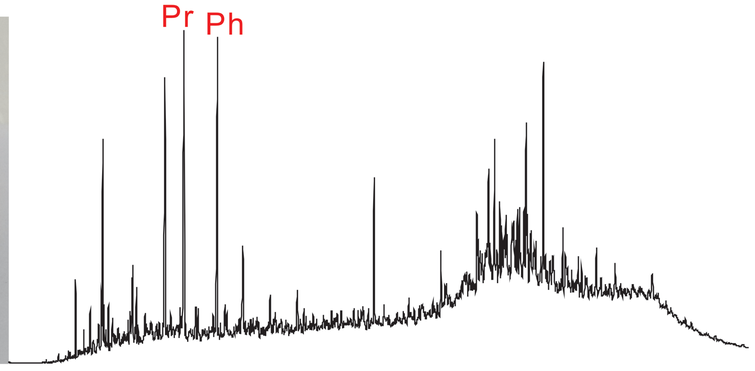

(i)Al-40

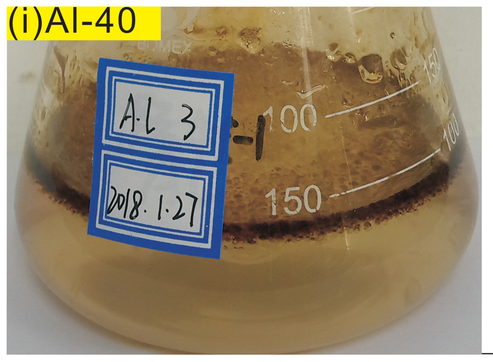

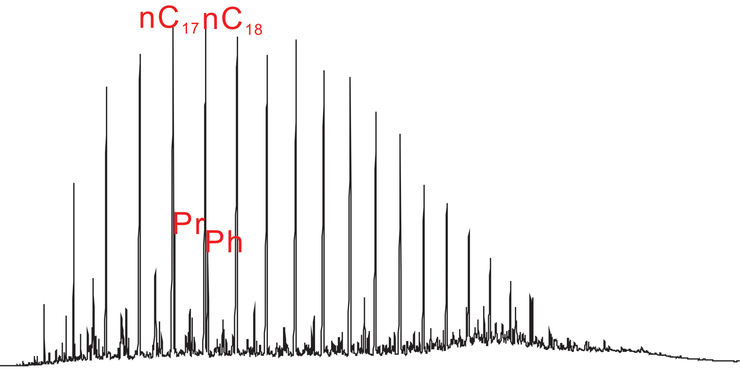

(j)Pa-60

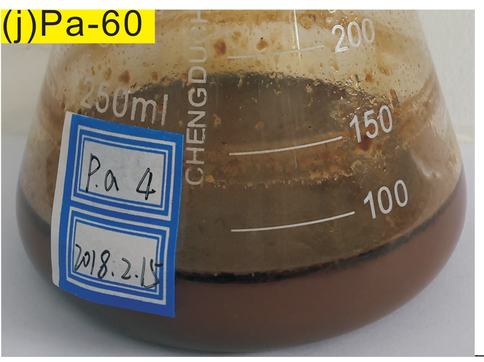

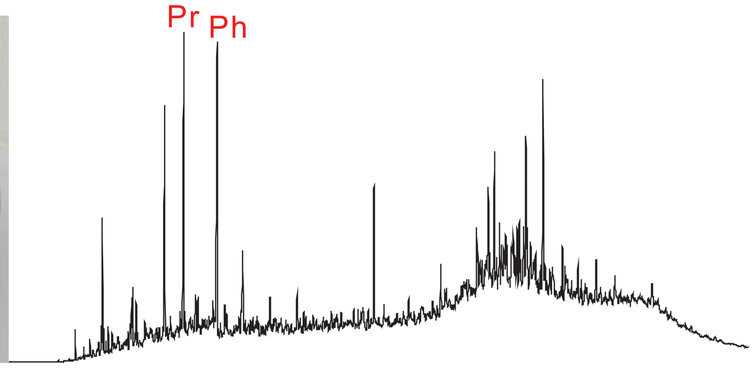

(k)Al-60

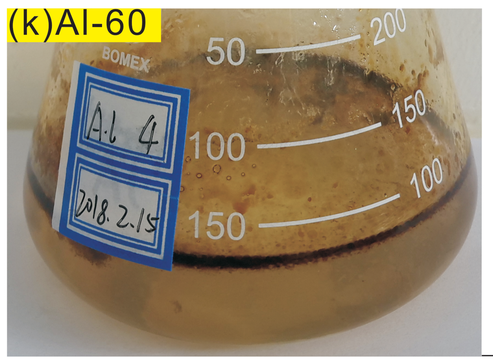

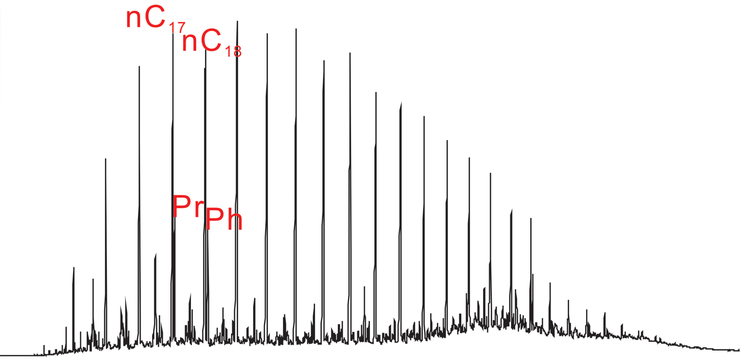

(l)Pa-90

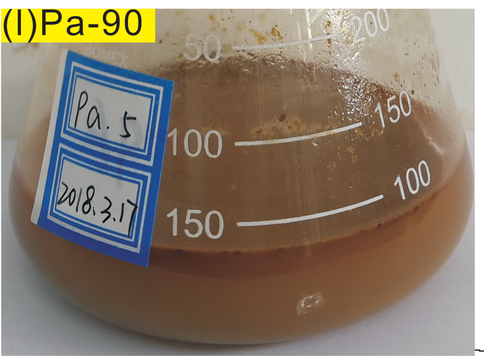

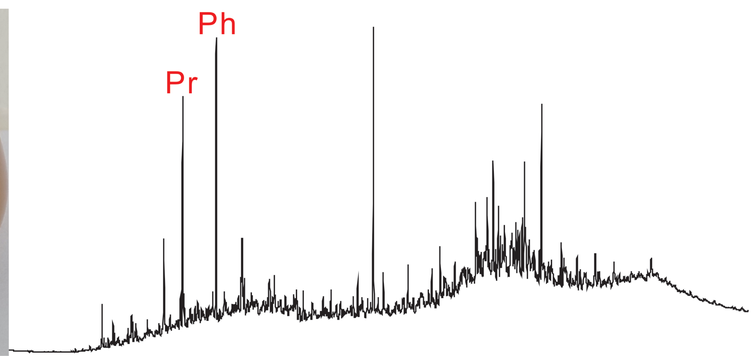

(m)Al-90

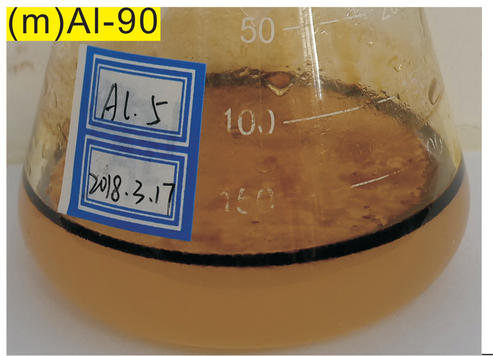

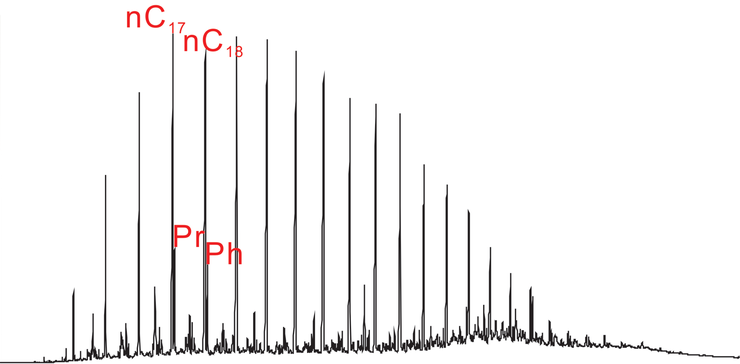

Figure 2.

(a)

Concentration(μg/g)

0
1000
2000
3000
4000
5000
6000
7000
8000

Oil
Pa-10
Pa-20
Pa-40
Pa-60
Pa-90

(b)

Concentration(μg/g)

0
1000
2000
3000
4000
5000
6000
7000
8000

Oil
Al-10
Al-20
Al-40
Al-60
Al-90

nC14 nC15 nC16 nC17 nC18 nC19 nC20 nC21 nC22 nC23 nC24 nC25 nC26 nC27 nC28 nC29 nC30 nC31 nC32 nC33 nC34 nC35

Figure 3.

(a)

Concentration(μg/g)

700
600
500
400
300
200
100
0

Oil
Pa-10
Pa-20
Pa-40
Pa-60
Pa-90

(b)

Concentration(μg/g)

700
600
500
400
300
200
100
0

Oil
Al-10
Al-20
Al-40
Al-60
Al-90

nC8-cHex
nC9-cHex
nC10-cHex
nC11-cHex
nC12-cHex
nC13-cHex
nC14-cHex
nC15-cHex
nC16-cHex
nC17-cHex
nC18-cHex
nC19-cHex
nC20-cHex
nC21-cHex
nC22-cHex
nC23-cHex
nC24-cHex
nC25-cHex
nC26-cHex
nC27-cHex
nC28-cHex
nC29-cHex
nC30-cHex
nC31-cHex

Figure 4.

(a)

Oil
Pa-10
Pa-20
Pa-40
Pa-60
Pa-90

Concentration(μg/g)

300
250
200
150
100
50
0

(b)

Oil
Al-10
Al-20
Al-40
Al-60
Al-90

Concentration(μg/g)

300
250
200
150
100
50
0

1 2 3 4 5 6 7 8 9 10 11

Figure 5.

(a)

Oil
Pa-10
Pa-20
Pa-40
Pa-60
Pa-90

Concentration(μg/g)

0
20
40
60
80
100

(b)

Oil
Al-10
Al-20
Al-40
Al-60
Al-90

Concentration(μg/g)

0
20
40
60
80
100

1 2 3 4 5 6 7 8 9 10 11 12 13 14 15 16 17 18 19 20

Figure 6.

(a)

Concentration(μg/g)

1000
800
600
400
200
0

Oil
Pa-10
Pa-20
Pa-40
Pa-60
Pa-90

(b)

Concentration(μg/g)

1000
800
600
400
200
0

Oil
Al-10
Al-20
Al-40
Al-60
Al-90

2
4
6
8
10
12
14
16
18
20

Figure 7.

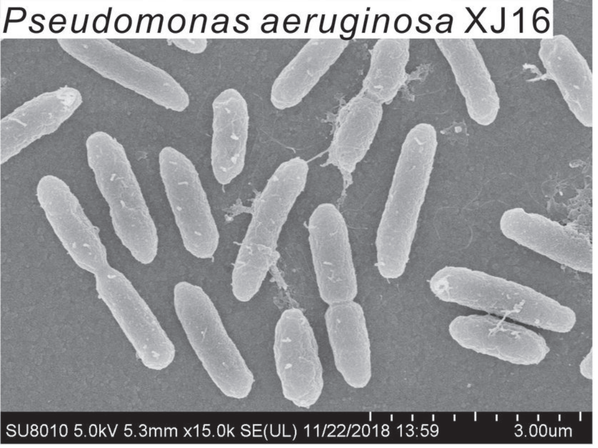

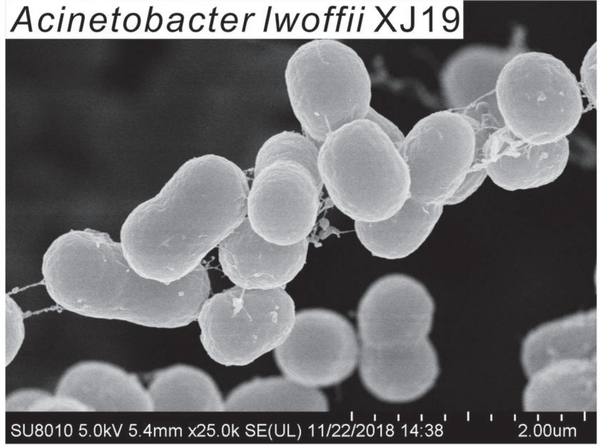

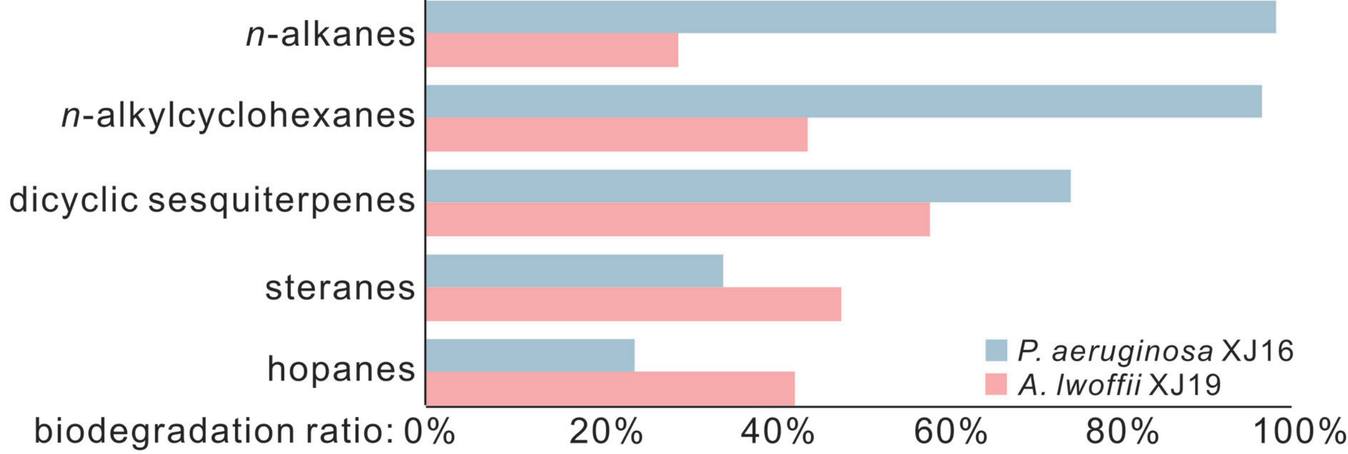

Different biodegradation sequences

P. aeruginosa XJ16

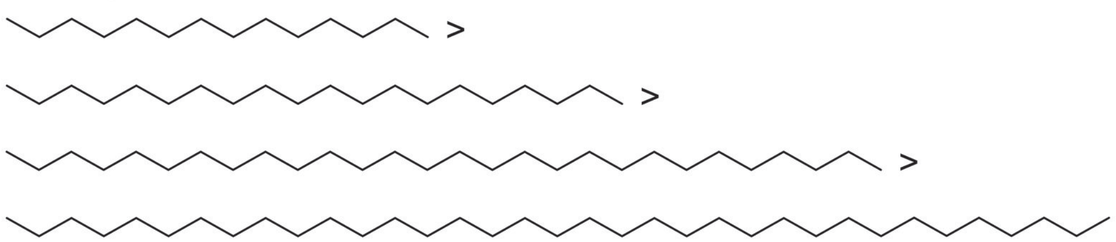

P. aeruginosa XJ16

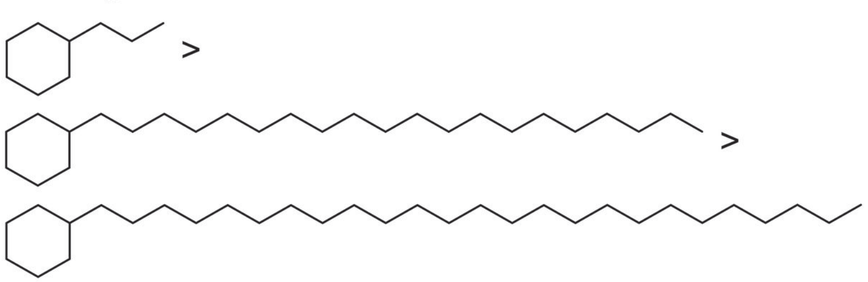

A. lwoffii XJ19

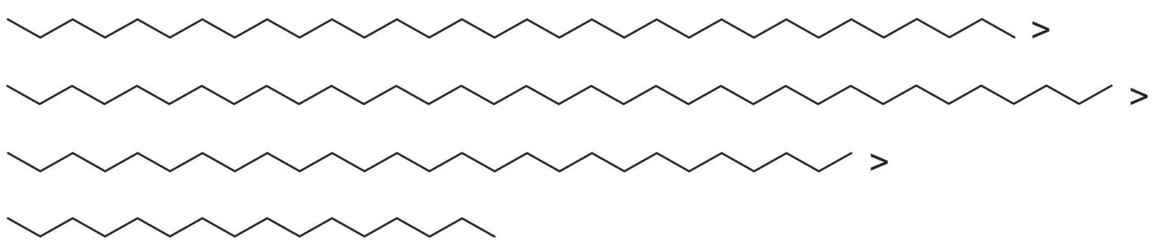

A. lwoffii XJ19

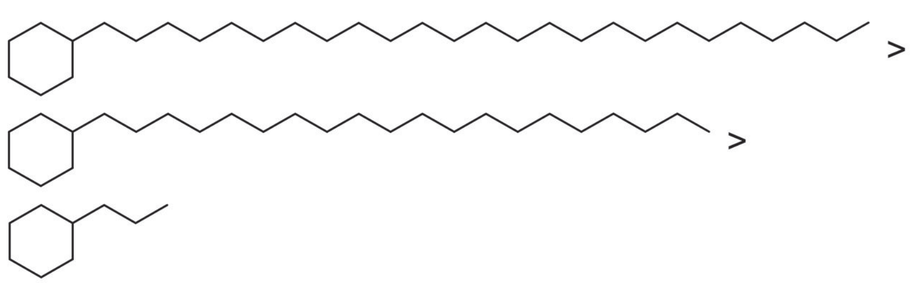

Same biodegradation sequences

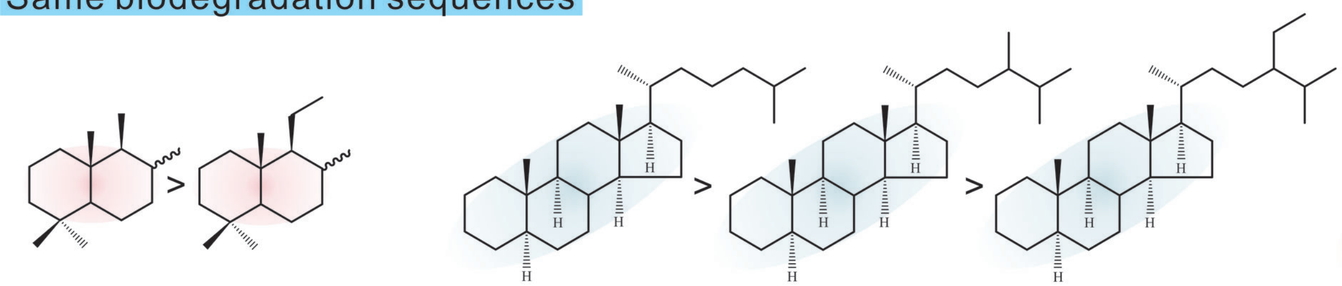

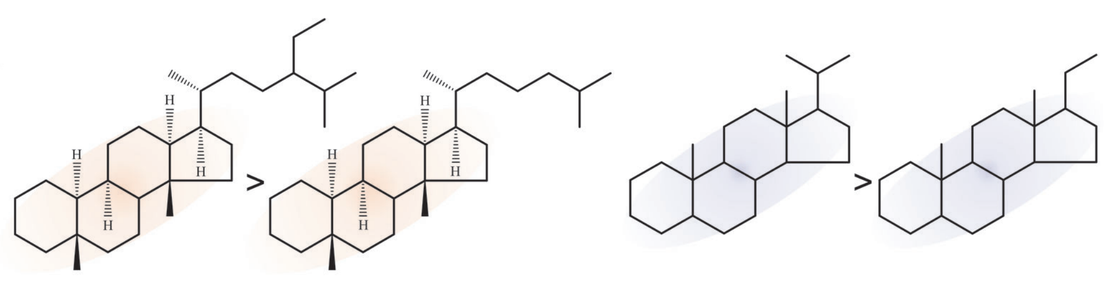

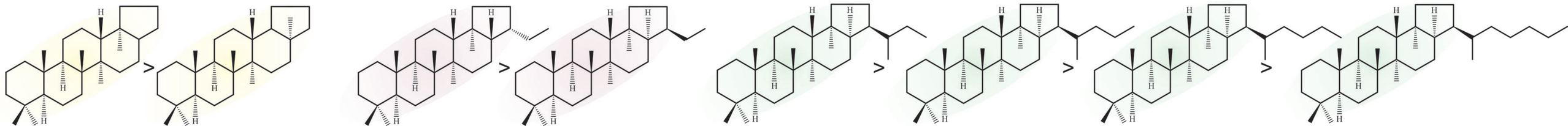

Table 1. Change of the biodegradation ratio (%) and four fractions (%) during biodegradation

	Biodegradation time (day)	Biodegradation ratio (%)	SARA (wt %)				
			Saturate	Aromatics	Resin	Asphaltene	Recovery(%)
Oil	0	0.0	77.4	14.9	5.3	2.5	89.0
Pa-10	10	47.1	65.2	20.5	10.0	4.3	96.1
Pa-20	20	55.3	70.1	17.8	8.5	3.6	90.2
Pa-40	40	61.8	68.2	17.9	8.8	5.2	90.9
Pa-60	60	65.3	67.1	19.6	12.6	0.7	95.7
Pa-90	90	69.3	69.1	18.0	9.4	3.4	95.1
Al-10	10	20.9	73.8	14.6	7.7	3.8	92.5
Al-20	20	21.6	77.5	14.3	6.7	1.4	96.7
Al-40	40	22.1	74.8	15.3	8.3	1.7	94.2
Al-60	60	32.3	75.7	13.6	9.4	1.3	97.9
Al-90	90	33.2	67.7	16.4	11.1	4.8	99.5

Table 2. Removal of *n*-alkanes via biodegradation by *P. aeruginosa* XJ16 and *A. lwoffii* XJ19

m/*z* 85			Concentration (μg/g)						Biodegradation	Concentration (μg/g)					Biodegradation
Number	Compound	Abbreviation	Oil	Pa-10	Pa-20	Pa-40	Pa-60	Pa-90	ratio (%)	Al-10	Al-20	Al-40	Al-60	Al-90	ratio (%)
1	nC_{14}-alkane	nC_{14}	3169.9	26.4	13.3	12.1	7.5	7.2	99.8	3042.0	3479.6	1955.7	762.6	587.4	81.5
2	nC_{15}-alkane	nC_{15}	5143.0	61.9	43.7	41.2	31.6	29.5	99.4	5433.0	5495.7	4126.4	2458.7	2273.9	55.8
3	nC_{16}-alkane	nC_{16}	5998.6	51.2	34.9	27.8	25.4	19.8	99.7	6379.2	6175.1	5713.1	4214.7	4094.9	31.7
4	nC_{17}-alkane	nC_{17}	6801.6	64.2	48.9	47.4	47.0	48.1	99.3	7048.8	6730.2	6976.5	5844.0	5798.8	14.7
5	nC_{18}-alkane	nC_{18}	6881.1	42.2	26.5	23.2	30.9	25.6	99.6	7007.6	6432.9	7174.5	6368.0	6258.0	9.1
6	nC_{19}-alkane	nC_{19}	7017.1	120.1	69.1	70.3	67.9	63.2	99.1	6578.2	6411.0	6808.3	6107.8	5942.8	15.3
7	nC_{20}-alkane	nC_{20}	6948.5	42.2	33.5	26.4	25.8	26.5	99.6	6514.6	6373.7	6662.3	6065.1	5982.0	13.9
8	nC_{21}-alkane	nC_{21}	6940.1	38.6	38.0	31.2	37.3	31.0	99.6	6419.6	6343.0	6537.0	6061.7	5934.8	14.5
9	nC_{22}-alkane	nC_{22}	6310.3	51.3	78.8	66.4	65.7	19.7	99.7	5761.8	5523.0	5784.4	5445.1	5364.0	15.0
10	nC_{23}-alkane	nC_{23}	6188.6	51.5	30.7	41.1	40.3	37.3	99.4	5504.6	5353.5	5430.9	5238.3	5056.4	18.3
11	nC_{24}-alkane	nC_{24}	5546.9	132.8	80.1	81.8	78.9	34.6	99.4	4742.8	4546.5	4487.8	4620.4	4303.8	22.4
12	nC_{25}-alkane	nC_{25}	5263.9	70.8	106.7	98.3	106.3	52.1	99.0	4454.9	4238.7	3879.8	3860.1	3831.1	27.2
13	nC_{26}-alkane	nC_{26}	4455.4	48.2	55.7	55.6	57.1	21.0	99.5	3647.9	3420.4	2901.1	2910.5	2938.3	34.0
14	nC_{27}-alkane	nC_{27}	4122.8	27.9	47.9	41.9	47.5	11.5	99.7	3201.4	2966.5	2293.5	2302.4	2416.5	41.4
15	nC_{28}-alkane	nC_{28}	3334.7	34.8	51.8	37.0	29.0	32.3	99.0	2396.1	2146.1	1490.7	1563.8	1693.1	49.2
16	nC_{29}-alkane	nC_{29}	2821.7	101.8	78.1	60.1	70.1	40.0	98.6	1966.5	1725.9	1159.0	1296.0	1218.9	56.8
17	nC_{30}-alkane	nC_{30}	2016.9	108.7	101.0	94.9	99.1	74.9	96.3	1299.3	1085.5	689.0	758.8	827.7	59.0
18	nC_{31}-alkane	nC_{31}	1530.2	77.8	71.5	59.2	62.7	44.2	97.1	874.3	742.5	427.9	430.1	537.5	64.9
19	nC_{32}-alkane	nC_{32}	946.9	36.1	42.8	37.6	33.4	26.7	97.2	444.2	362.9	205.6	231.7	255.9	73.0
20	nC_{33}-alkane	nC_{33}	704.1	118.7	115.3	137.7	128.9	127.7	81.9	287.3	212.3	241.7	221.5	179.5	74.5

21	nC_{34}-alkane	nC_{34}	555.9	191.7	209.4	182.5	177.9	190.8	65.7	209.6	175.5	193.3	180.0	179.5	67.7
22	nC_{35}-alkane	nC_{35}	364.0	131.0	120.6	113.1	139.7	144.7	60.2	157.8	136.3	143.0	140.7	136.2	62.6
Total concentration (μg/g)			93062.3	1629.7	1498.1	1386.6	1409.7	1108.5		83371.7	80077.0	75281.3	67082.0	65811.1	
Total biodegradation ratio (%)				98.2	98.4	98.5	98.5	98.8		10.4	14.0	19.1	27.9	29.3	

2

Table 3. Removal of *n*-alkylcyclohexanes via biodegradation by *P. aeruginosa* XJ16 and *A. lwoffii* XJ19

m/*z* 82			Concentration (μg/g)						Biodegradation	Concentration (μg/g)					Biodegradation
Number	Compound	Abbreviation	Oil	Pa-10	Pa-20	Pa-40	Pa-60	Pa-90	ratio (%)	Al-10	Al-20	Al-40	Al-60	Al-90	ratio (%)
1	nC_8-alkyl cyclohexane	nC_8-cHex	23.5	14.1	19.6	4.8	6.3	6.4	72.7	46.2	71.8	123.1	44.4	17.2	26.8
2	nC_9-alkyl cyclohexane	nC_9-cHex	167.4	81.2	13.8	27.2	6.1	18.2	89.1	173.0	207.2	266.0	174.2	96.0	42.6
3	nC_{10}-alkyl cyclohexane	nC_{10}-cHex	401.7	76.1	7.5	18.6	5.7	6.5	98.4	330.9	351.8	456.0	394.1	277.8	30.8
4	nC_{11}-alkyl cyclohexane	nC_{11}-cHex	545.4	83.9	26.3	20.8	20.2	17.9	96.7	466.2	474.6	420.5	391.3	315.7	42.1
5	nC_{12}-alkyl cyclohexane	nC_{12}-cHex	577.8	63.0	17.5	12.2	6.9	4.5	99.2	441.1	426.9	467.8	467.4	391.2	32.3
6	nC_{13}-alkyl cyclohexane	nC_{13}-cHex	601.8	29.7	5.5	7.6	9.5	6.6	98.9	468.0	389.4	442.0	447.5	383.2	36.3
7	nC_{14}-alkyl cyclohexane	nC_{14}-cHex	587.9	41.4	19.0	14.2	18.0	12.1	97.9	416.5	404.5	365.0	375.3	324.2	44.8
8	nC_{15}-alkyl cyclohexane	nC_{15}-cHex	466.5	39.3	14.0	11.8	13.5	9.6	97.9	340.1	330.2	295.8	292.7	264.2	43.4
9	nC_{16}-alkyl cyclohexane	nC_{16}-cHex	474.6	27.7	15.7	8.2	9.2	2.2	99.5	289.3	284.9	279.9	271.3	255.4	46.2
10	nC_{17}-alkyl cyclohexane	nC_{17}-cHex	438.1	46.7	21.3	7.9	13.0	3.2	99.3	270.6	257.4	239.1	236.7	217.2	50.4
11	nC_{18}-alkyl cyclohexane	nC_{18}-cHex	397.9	37.2	7.8	9.7	7.6	2.6	99.4	237.0	221.2	239.7	233.1	233.3	41.4
12	nC_{19}-alkyl cyclohexane	nC_{19}-cHex	401.5	61.0	11.1	18.6	21.2	0.8	99.8	233.5	223.4	259.2	220.2	210.4	47.6
13	nC_{20}-alkyl cyclohexane	nC_{20}-cHex	408.8	66.1	29.6	10.9	20.6	0.8	99.8	227.2	214.0	254.7	247.1	241.7	40.9
14	nC_{21}-alkyl cyclohexane	nC_{21}-cHex	427.8	127.9	83.3	69.1	76.2	61.3	85.7	246.4	228.1	253.4	249.3	245.9	42.5
15	nC_{22}-alkyl cyclohexane	nC_{22}-cHex	453.7	119.6	67.0	19.7	56.9	7.2	98.4	245.0	228.9	287.7	289.2	289.1	36.3
16	nC_{23}-alkyl cyclohexane	nC_{23}-cHex	482.6	117.4	36.0	29.7	29.6	44.5	90.8	280.0	269.3	248.1	271.7	254.3	47.3
17	nC_{24}-alkyl cyclohexane	nC_{24}-cHex	489.7	110.5	48.1	32.6	36.0	11.3	97.7	244.9	258.4	286.7	368.0	302.2	38.3
18	nC_{25}-alkyl cyclohexane	nC_{25}-cHex	365.6	100.9	40.2	17.1	22.7	3.2	99.1	331.5	323.2	216.2	297.1	234.2	35.9
19	nC_{26}-alkyl cyclohexane	nC_{26}-cHex	328.9	104.6	46.9	27.9	29.1	18.7	94.3	278.6	256.9	138.3	156.9	147.1	55.3
20	nC_{27}-alkyl cyclohexane	nC_{27}-cHex	298.3	114.2	46.6	18.8	23.8	2.9	99.0	170.6	155.2	109.2	138.3	123.8	58.5

21	nC_{28}-alkyl cyclohexane	nC_{28}-cHex	242.0	72.2	33.5	7.7	18.8	0.8	99.7	133.2	121.9	114.4	168.7	128.3	47.0
22	nC_{29}-alkyl cyclohexane	nC_{29}-cHex	281.6	65.6	31.0	20.0	12.2	0.5	99.8	146.0	132.9	57.4	94.2	65.3	76.8
23	nC_{30}-alkyl cyclohexane	nC_{30}-cHex	159.0	62.2	55.2	49.6	52.1	11.0	93.1	75.1	64.9	38.2	80.5	47.2	70.3
24	nC_{31}-alkyl cyclohexane	nC_{31}-cHex	156.1	37.4	16.1	11.7	11.1	10.0	93.6	66.2	55.4	45.2	74.5	49.1	68.6
Total concentration (μg/g)			9178.0	1699.9	712.6	476.3	526.4	262.9		6157.1	5952.4	5903.7	5983.9	5114.1	
Total biodegradation ratio (%)				81.5	92.2	94.8	94.3	97.1		32.9	35.1	35.7	34.8	44.3	

2

Table 4. Removal of bicyclic sesquiterpenes via biodegradation by *P. aeruginosa* XJ16 and *A. lwoffii* XJ19

m/*z* 123		Concentration (μg/g)						Biodegradation	Concentration (μg/g)					Biodegradation
Number	Compound	Oil	Pa-10	Pa-20	Pa-40	Pa-60	Pa-90	ratio (%)	Al-10	Al-20	Al-40	Al-60	Al-90	ratio (%)
1	C_{14}-bicyclic sesquiterpene	22.9	22.3	12.5	6.4	1.2	0.6	97.4	20.2	19.2	20.8	13.9	5.7	74.9
2	C_{14}-bicyclic sesquiterpene	27.2	29.6	16.7	9.5	2.6	1.3	95.2	40.2	39.5	35.5	17.0	7.3	73.2
3	C_{15}-bicyclic sesquiterpene	174.7	169.6	108.9	77.5	39.1	21.3	87.8	175.3	174.9	160.7	115.5	58.1	66.8
4	C_{15}-bicyclic sesquiterpene	202.6	192.0	130.3	106.2	60.3	37.4	81.5	195.9	182.0	171.0	139.1	78.1	61.4
5	8α(H)-drimane	219.7	194.0	136.7	116.7	72.4	47.3	78.5	211.0	200.2	189.0	162.5	87.9	60.0
6	8β(H)-drimane	169.6	139.4	98.1	84.6	52.6	34.2	79.8	146.3	150.0	134.8	117.1	63.5	62.6
7	C_{15}-bicyclic sesquiterpene	61.9	76.4	54.3	49.7	32.1	22.0	64.4	71.5	67.5	58.1	52.4	36.1	41.7
8	C_{16}-bicyclic sesquiterpene	29.5	33.5	24.5	30.9	19.6	10.8	63.4	36.2	28.3	13.0	31.4	12.0	59.2
9	C_{15}-bicyclic sesquiterpene	118.9	102.5	77.6	78.1	58.1	44.0	63.0	106.9	107.9	99.3	96.5	59.2	50.2
10	C_{16}-bicyclic sesquiterpene	62.0	51.3	33.2	35.8	26.1	19.5	68.5	49.7	48.4	40.4	41.2	24.7	60.3
11	8β(H)-homodrimane	238.0	204.0	145.9	150.3	120.3	95.1	60.0	198.1	201.8	185.2	187.2	117.8	50.5
Total concentration (μg/g)		1327.1	1214.7	838.8	745.7	484.2	333.6		1251.2	1219.7	1107.9	973.9	550.5	
Total biodegradation ratio (%)			8.5	36.8	43.8	63.5	74.9		5.7	8.1	16.5	26.6	58.5	

Table 5. Removal of steranes via biodegradation by *P. aeruginosa* XJ16 and *A. lwoffii* XJ19

	m/z 217		Concentration (μg/g)						Biodegradation	Concentration (μg/g)					Biodegradation
Number	Compound	Abbreviation	Oil	Pa-10	Pa-20	Pa-40	Pa-60	Pa-90	ratio (%)	Al-10	Al-20	Al-40	Al-60	Al-90	ratio (%)
1	C_{21}-5α(H)-pregnane		27.6	20.3	20.2	20.1	21.7	18.7	32.3	21.1	21.2	22.6	20.6	18.7	32.2
2	C_{22}-5α(H)-homopregnane		14.8	8.0	8.4	8.0	8.7	7.9	46.9	10.0	11.1	9.9	8.8	8.1	45.4
3	13β(H),17α(H)-C_{27}diastrane(20S)	βαC_{27}20S	24.9	20.8	18.0	18.5	17.1	16.9	32.0	14.2	13.9	16.0	15.4	14.3	42.5
4	13β(H),17α(H)-C_{27}diastrane(20R)	βαC_{27}20R	11.4	8.2	8.4	10.6	8.1	8.2	27.5	8.9	7.4	7.6	5.4	8.4	25.9
5	13α(H),17β(H)-C_{27}diastrane(20S)	αβC_{27}20S	4.6	4.3	5.2	4.0	3.3	3.3	26.8	3.1	2.5	3.7	3.0	3.2	29.5
6	13α(H),17β(H)-C_{27}diastrane(20R)	αβC_{27}20R	5.8	5.8	5.0	5.7	6.9	3.8	34.2	3.3	2.5	5.7	4.0	6.3	-8.7
7	5α(H),14α(H),17α(H)-sterane(20S)	αααC_{27}20S	38.8	34.4	27.1	25.2	26.2	23.5	39.3	24.1	22.3	23.0	22.4	22.0	43.3
8	5α(H),14β(H),17β(H)-sterane(20R)	αββC_{27}20R	72.7	62.7	52.0	46.9	45.5	44.1	39.3	40.3	40.1	37.6	38.0	36.7	49.5
9	5α(H),14β(H),17β(H)-sterane(20S)	αββC_{27}20S	60.0	58.5	45.8	38.1	39.1	38.5	35.9	36.6	37.8	32.5	35.5	30.8	48.8
10	5α(H),14α(H),17α(H)-sterane(20R)	αααC_{27}20R	63.9	20.1	19.1	20.3	19.6	23.3	63.6	17.8	18.2	16.5	16.0	14.9	76.7
11	13β(H),17α(H)-C_{29}diastrane(20R)	βαC_{29}20R	13.8	11.6	10.1	9.5	10.6	5.0	63.5	8.5	8.2	7.4	6.9	7.1	48.3
12	13α(H),17β(H)-C_{29}diastrane(20S)	αβC_{29}20S	29.5	7.1	8.2	7.3	7.2	6.9	76.7	5.9	6.0	7.0	5.8	6.2	78.9
13	24-methyl-5α(H),14α(H),17α(H)-sterane(20S)	αααC_{28}20S	24.1	18.4	17.5	16.8	15.2	14.6	39.5	11.1	11.7	12.7	13.1	11.7	51.6
14	24-methyl-5α(H),14β(H),17β(H)-sterane(20R)	αββC_{28}20R	77.0	65.2	64.4	61.4	54.9	53.3	30.7	47.6	47.3	49.0	48.7	47.5	38.3
15	24-methyl-5α(H),14β(H),17β(H)-sterane(20S)	αββC_{28}20S	87.7	80.3	74.8	65.6	64.7	63.1	28.1	51.6	50.4	50.5	52.3	48.7	44.5
16	24-methyl-5α(H),14α(H),17α(H)-sterane(20R)	αααC_{28}20R	60.2	39.3	36.4	33.4	31.7	31.3	48.0	26.4	26.5	25.3	23.8	24.1	59.9
17	24-ethyl-5α(H),14α(H),17α(H)-sterane(20S)	αααC_{29}20S	78.9	62.9	54.0	60.0	47.6	47.3	40.1	41.5	40.5	36.3	34.8	36.7	53.5
18	24-ethyl-5α(H),14β(H),17β(H)-sterane(20R)	αββC_{29}20R	91.6	87.5	86.2	76.1	71.6	71.9	21.5	53.7	51.7	51.8	49.9	49.4	46.1
19	24-ethyl-5α(H),14β(H),17β(H)-sterane(20S)	αββC_{29}20S	76.2	75.3	75.3	68.3	65.5	66.3	13.0	49.0	47.8	46.5	45.7	45.3	40.5
20	24-ethyl-5α(H),14α(H),17α(H)-sterane(20R)	αααC_{29}20R	61.5	64.9	63.5	58.8	59.4	57.7	6.2	39.5	38.2	40.4	38.7	39.1	36.4

Total concentration (μg/g)	924.9	755.4	699.7	654.6	624.6	605.7	514.2	505.3	502.0	488.7	479.3
Total biodegradation ratio (%)		18.3	24.4	29.2	32.5	34.5	44.4	45.4	45.7	47.2	48.2

2

1 Table 6. Removal of hopanes via biodegradation by *P. aeruginosa* XJ16 and *A. lwoffii* XJ19

m/z 191			Concentration (μg/g)						Biodegradation	Concentration (μg/g)					Biodegradation
Number	Compound	Abbreviation	Oil	Pa-10	Pa-20	Pa-40	Pa-60	Pa-90	ratio (%)	Al-10	Al-20	Al-40	Al-60	Al-90	ratio (%)
1	18α(H)-22,29,30-trisnorneohopane	Ts	155.0	132.0	122.4	115.5	108.8	109.5	29.3	84.2	83.1	86.0	85.5	81.7	47.3
2	17α(H)-22,29,30-trisnorhopane	Tm	131.3	85.3	76.0	65.5	58.7	64.0	51.3	53.1	52.5	55.3	54.9	53.4	59.3
3	17α,21β(H)-30 norhopane	$C_{29}H$	384.9	380.5	356.0	311.2	310.2	299.7	22.1	210.8	208.1	224.2	223.8	219.9	42.9
4	18α,21β(H)-30 norneohopane	$C_{29}Ts$	116.3	111.0	119.1	116.5	113.2	107.6	7.5	73.9	71.4	86.3	85.3	80.7	30.6
5	C_{30} diahopane	C_{30}*	119.5	88.1	111.2	86.9	101.3	92.0	23.0	68.3	67.4	62.4	71.1	72.8	39.1
6	17β(H),21α(H)-30 normoretane	$C_{29}M$	33.3	28.3	17.0	15.9	21.4	14.0	57.8	11.9	11.4	15.1	14.0	15.3	54.1
7	18α(H)-oleanane	Ol	34.7	27.6	20.9	14.0	21.2	10.1	70.8	12.9	12.3	13.7	14.2	12.7	63.3
8	17α(H),21β(H)-hopane	$C_{30}H$	833.6	769.2	748.5	686.7	679.6	651.3	21.9	444.9	439.5	450.2	446.1	443.0	46.8
9	17β(H),21α(H)-moretane	$C_{30}M$	77.4	70.8	66.4	53.9	56.2	54.2	30.0	38.2	40.3	42.7	43.3	42.5	45.0
10	17α(H),21β(H)-30 homohopane(22S)	$C_{31}H22S$	159.1	146.5	139.4	121.6	116.4	114.2	28.3	83.2	80.4	89.9	91.3	89.6	43.7
11	17α(H),21β(H)-30 homohopane(22R)	$C_{31}H22R$	147.4	89.8	110.6	95.2	93.0	85.1	42.2	59.3	62.8	72.3	78.5	76.6	48.0
12	Gammacerane	Gam	24.9	27.0	38.3	33.1	31.9	27.8	-11.8	18.4	18.1	23.7	27.2	27.4	-10.4
13	17β(H),21α(H)-30 homomoretane(22S+22R)		16.4	16.8	23.1	24.2	22.7	18.7	-13.8	16.1	16.2	18.6	23.7	19.4	-18.5
14	17α(H),21β(H)-30,31 dihomohopane(22S)	$C_{32}H22S$	109.7	91.8	103.6	92.7	84.5	84.3	23.2	64.8	61.7	67.5	71.5	69.9	36.3
15	17α(H),21β(H)-30,31 dihomohopane(22R)	$C_{32}H22R$	87.1	70.6	65.6	60.4	53.4	59.0	32.3	41.7	38.8	45.2	48.5	44.8	48.5
16	17α(H),21β(H)-30,31 ,32 trihomohopane(22S)	$C_{33}H22S$	65.1	61.3	76.6	67.4	65.1	65.2	0.0	42.5	40.4	47.5	48.9	48.6	25.4
17	17α(H),21β(H)-30,31 ,32trihomohopane(22R)	$C_{33}H22R$	44.4	43.0	42.7	42.2	35.1	36.2	18.5	25.2	23.8	29.8	30.3	30.8	30.5
18	17α(H),21β(H)-30,31 ,32 ,33 tetrahomohopane(22S)	$C_{34}H22S$	37.7	39.4	54.9	46.6	39.2	42.0	-11.4	26.6	24.6	31.4	28.1	28.5	24.5
19	17α(H),21β(H)-30,31 ,32 ,33 tetrahomohopane(22R)	$C_{34}H22R$	22.9	22.3	30.0	31.2	25.9	26.6	-16.1	17.8	16.0	24.2	19.7	22.8	0.2
20	17α(H),21β(H)-30,31 ,32 ,33 ,34 pentahomohopane(22S)	$C_{35}H22S$	22.7	22.8	20.0	18.0	17.6	16.0	29.4	9.6	9.1	12.4	12.4	12.5	45.1

21	17α(H),21β(H)-30,31 ,32 ,33 ,34 pentahomohopane(22R)	C_{35}H22R	12.8	14.0	20.5	22.7	22.0	19.7	-53.1	11.8	9.2	14.0	14.6	14.5	-12.8
Total concentration (μg/g)			2636.2	2337.9	2363.0	2121.5	2077.4	1997.1		1415.2	1387.1	1512.5	1532.5	1507.7	
Total biodegradation ratio (%)				11.3	10.4	19.5	21.2	24.2		46.3	47.4	42.6	41.9	42.8	